Soft Matter

REVIEW

Fibrous polymer nanomaterials for biomedical applications and their transport by fluids: an overview

Cite this: DOI: 10.1039/c8sm01269e

S. Pawłowska, T. A. Kowalewski and F. Pierini

Over the past few decades, there has been strong interest in the development of new micro- and nanomaterials for biomedical applications. Their use in the form of capsules, particles or filaments suspended in body fluids is associated with conformational changes and hydrodynamic interactions responsible for their transport. The dynamics of fibres or other long objects in Poiseuille flow is one of the fundamental problems in a variety of biomedical contexts, such as mobility of proteins, dynamics of DNA or other biological polymers, cell movement, tissue engineering, and drug delivery. In this review, we discuss several important applications of micro and nanoobjects in this field and try to understand the problems of their transport in flow resulting from material-environment interactions in typical, crowded, and complex biological fluids. Our aim is to elucidate the relationship between the nano- and microscopic structures of elongated polymer particles and their flow properties, thus opening the possibility to design nanoobjects that can be efficiently transported by body fluids for targeted drug release or local tissue regeneration.

Received 21st June 2018,
Accepted 10th October 2018

DOI: 10.1039/c8sm01269e

rsc.li/soft-matter-journal

Introduction

In recent years growing attention has been paid to the functioning of large molecular systems which are typical of biological environments (Fig. 1(a and b)).[1] It has appeared that despite the high degree of crowding in such systems, the mobility of single molecules of nano- and micromaterials plays a decisive role in understanding their role as transporters and signalling envoys at the cellular level. Physical forces that interact in a confined space include van der Waals, electrostatic, and excluded volume interactions (Fig. 1(c)). Advances in the modelling of polymers have improved the understanding of some of these aspects (Fig. 1(d)). Even the recent atomistic model of whole living cells,[2] however, is unable to cover time and space scales which are significant for analysing experimental observations. On the other hand, the simplified coarse-grained models miss several important aspects such as, for example, the high content of water molecules in any biological environment.

The interaction of flexible polymers with fluid flow leads to a number of nontrivial phenomena. Their interpretation in terms

Institute of Fundamental Technological Research, Polish Academy of Sciences, Pawinskiego 5B, 02-106 Warsaw, Poland. E-mail: spaw@ippt.pan.pl

S. Pawłowska

Sylwia Pawłowska graduated in biotechnology from the Gdansk University of Technology. In 2013 she started her PhD at the Institute of Fundamental Technological Research (IPPT PAN). In 2018 she submitted her thesis on dynamics of nano objects suspended in liquids. She has authored or co-authored six papers in the area of bioengineering, dynamics of macromolecules, and medical applications of nanofibres.

T. A. Kowalewski

Tomasz Aleksander Kowalewski graduated from Faculty of Physics at Warsaw University in 1969. His PhD and habilitation were obtained from the Institute of Fundamental Technological Research (IPPT PAN). Presently, he is a full professor at IPPT PAN. His main research interests are fluid mechanics, bioengineering, and soft matter physics.

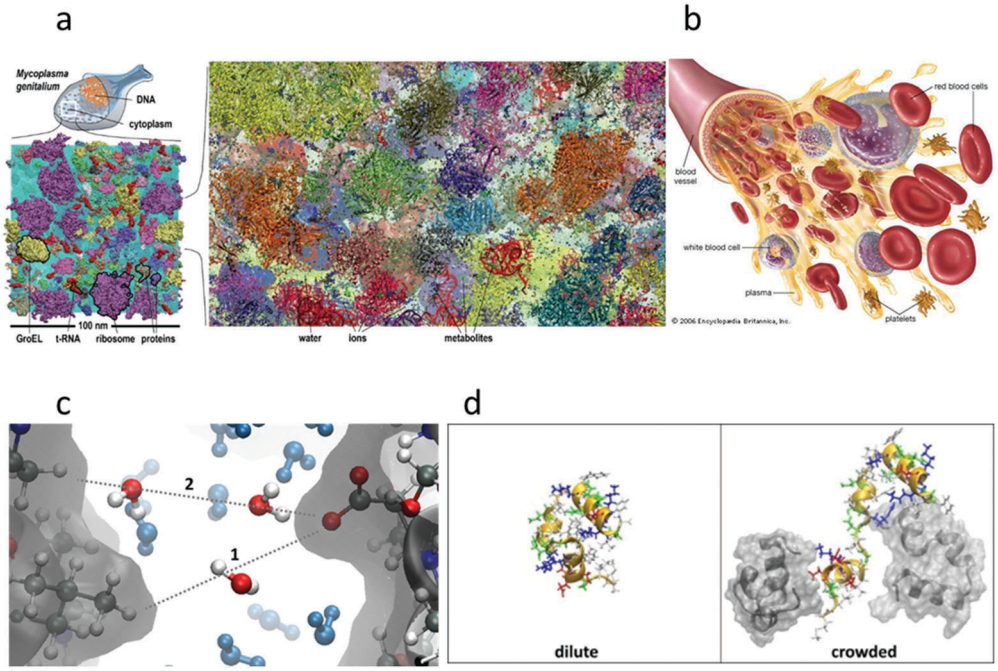

Fig. 1 Crowded environments: (a) in cytoplasm; (b) in the bloodstream; (c) interaction of protein and water molecules under crowded conditions; and (d) conformation of a biomolecule in dilute and crowded environment conditions. Image (a) is reprinted from Yu *et al.*[1] with permission. Image (b) is reprinted by courtesy of Encyclopaedia Britannica, Inc., copyright 2006; used with permission.[4] Image (c) and (d) are reprinted from Feig *et al.*[2] with permission.

of simple models of hydrodynamic interactions appears to be irrelevant for understanding the behaviour of these systems. This is not only due to the high degree of complexity and crowding at the molecular level, which is responsible for a strongly non-linear response to acting hydrodynamic forces. Unfortunately, typical quasi-steady hydrodynamic models are missing the short time response of interaction at the level of molecules. Biological objects are far too complex to be approximated by either the ''hydrodynamic diameter'' or even worm-like chain (WLC) structures. And for that reason, the physical reality of biological structures is far beyond such approximations. For example, it is known that the order of amino-acid sequences in DNA chains affects their mechanical response and coiling properties. Also the elasticity of proteins is correlated with disorders which are responsible for their failed functionalities.[3]

The confining geometry entails additional constraints on the structure of the polymer suspensions. Depending on the environment, a polymer has to adopt its random coiled configuration, hence modifying our interpretation of its response to external hydrodynamic and atomistic forces. Biopolymers in cell nuclei respond to their environment by adjusting their size and shape, changing their mechanical properties from extended (unfolded) random structures to globular structures resembling nanoparticles. Additionally, crowding modifies their conformations by compressing polymer coils and stabilizing folded states. Molecular modelling of such systems may offer microscopic details on acting intermolecular forces. By evaluating the macroscopic properties of the computational model one can compare the macroscopic properties of the model system with the experimental measurements of the real system. However, coupling between both scales is not trivial due to the dominating (at microscales) stochasticity driven by diffusion transport. The question arises: where to set the time and space limits of our physical description of particle-environment interactions to make such a validation of the model trustful. As usual, the only reliable solution is a compromise between experimental limitations and the ability of the model to

F. Pierini

Filippo Pierini is a researcher in the Department of Biosystems and Soft Matter at the Institute of Fundamental Technological Research (IPPT). He received both his MSc and PhD degrees in chemical sciences from the University of Bologna. He performed his doctoral work in the Laboratory of Environmental and Biological Structural Chemistry in which he focused on understanding the relationship between the hierarchical structures and properties of electrospun nanofibers. He then moved to IPPT, where he took up the role of group leader (Pierini Research Group). His research interests embrace the development of functional polymer nanomaterials for biomedical and other applications.

offer insight into phenomena beyond its direct, short-scale predictions.

Physicists like to deal with simplifications, allowing for precise mathematical analyses. In the case of modelling diffusion problems, a simple geometry of solid, spherical particles is commonly used to interpret real life. The experimental techniques of observing single particles are well established, and the evaluation of their movements is straightforward. It can be performed either on a statistical basis, such as by Dynamic Light Scattering (DLS), or by using Nanoparticle Tracking Analysis (NTA) equipment. However, every rose has its thorns. As we will show in the following, even an obviously simple physical problem, the diffusion of a single particle, generates a plethora of questions and unsolved problems in the real world.

Some help comes from the new experimental tools made available in recent decades, such as optical tweezers, and confocal or total internal reflection microscopy. They may help to deal with picoNewton forces acting at nanometric distances between particles, and encapsulating their nano-environment boundaries. Nevertheless, the interpretation of the experimental results obtained in this way, in terms of molecular, ionic, steric, and hydrodynamic forces, is still a challenging task. Alas, in real life there are no spherical, solid particles. In the best case, small molecules could be seen as more or less symmetrical bodies with kinematic boundary conditions of difficult interpretation when interacting with the environment (*e.g.* slip or no-slip b.c.).

Biomolecules are far from such a simple model: they are usually long, flexible polymeric chains with an enormously growing number of possible conformations, and nearly infinite degrees of freedom for possible interactions with their ends, neighbouring objects, and solvent molecules.[5] Therefore, the characterization of the flexibility or stiffness of biomolecules and polymers is the basis for describing their vital role in biological activities.

To return to modelling, setting computer programs for such long, flexible objects brings us to agree with several necessary simplifications. Hence, complex molecular interactions with spherical subunits are described in a reduced way as spherical proteins or worm-like chains. Their dynamic structure is regarded as one of stiff or semiflexible chains. To specify the randomness of the chain deformation, the so-called ''persistence length'' is defined, being a measure of the chain stiffness or flexibility: the stiffer the chain, the larger the persistence length.

Observing by optical means the dynamics of flexible molecules suspended in a liquid one may evaluate their main mechanical properties, which are responsible for their complex behaviour, like the folding–unfolding sequences of polymeric chains. However, understanding their dynamics through direct optical observations is limited by the temporal resolution of available experimental tools. The solution we found is to create an experimental model based on synthetic objects, like hydrogel nanofilaments. Recently developed techniques offer some help by permitting the production of highly flexible fibres, with deformability and elasticity resembling those of long macromolecules. Their elongated shape and flexibility open new fields for prospective applications as drug carriers and tissue-rebuilding agents, thanks to their ability for direct targeting of body tissues.

During the development of nanomaterials for biomedical applications many efforts are usually made to characterize the chemical and morphological properties, and their biocompatibility, because the material interactions with body fluids become fundamental, especially when they are applied as drug delivery systems.

Our aim is to elucidate the problems caused by inter-particle interactions in a typical, crowded biological environment and to find some possible experimental tools useful for gaining knowledge on the transport properties of individual objects suspended therein for biomedical applications, focusing our attention on elongated polymer biomaterials.

The review article is organized as follows. The first section introduces the main points of the biomedical aspects of nano scale suspensions used for diagnostics and therapies. Second, we will give an account of the importance of precise knowledge of the material mechanic and transport properties. We will expand the problem description in the following chapter reviewing Brownian diffusion and mobility of nanoobjects. In the third section, we will concentrate on the methods used for fabricating polymeric nanofilaments. In the fourth section, we will review a few methods used to analyse nano suspensions, introducing a novel experimental technique based on the use of optical tweezers combined with an atomic force microscope. Finally, we will close by presenting some future perspectives for the development of new fibrous polymer materials for advanced biomedical applications.

Biomedical applications

In recent years, the development of medicine and biology research has relied more and more on the development of nanotechnologies. Currently, nanotechnology products approved for clinical use are relatively simple. As a whole, there is a lack of active targeting and triggered drug release components. Despite numerous studies, this technology has still not achieved a significant clinical impact on human health. The reason for this is complex and depends on the type of application.[6] Undoubtedly, the development of nanomedicine is an important factor in the search for new applications of nanomaterials.[7] Nanomedicine is defined as the application of nanotechnologies in medicine; it includes targeted drug delivery, diagnostics, biosensing, and imaging.[7–9] Polymer-based micro- and nanoparticles have been the subject of intense research and development in the pharmaceutical sector in recent decades.[7,10] Currently, the interest of researchers is focused on polymer fibres. In the case of these elongated micro- and nanoobjects, research is focused on two main issues, drug delivery systems and scaffolds for tissue engineering.[11,12]

In contrast to spherical objects, fibres have broad perspectives for biomedical applications, not only as drug delivery

systems, but also as scaffolds and dressings, as will be described in more detail later in this chapter. Thanks to their elongated shape, fibres of a diameter comparable to that of spherical objects have a larger surface area and bulk that can carry large doses of drugs.

One of the goals of today's material engineering is to design and create nanomaterials which can travel to a specific target site in the body and, once there, release the drug, monitor diseases, and work as biosensors. The shared surface and structure of nanomaterials must be designed to obtain an affinity to specific cells in order to be protected from immune cells.[13] There are four main routes for nanoobjects to enter the body: by mouth, inhalation, dermal transfer, and systemic intravenous injection. The mechanisms that permit micro- and nanomaterials to arrive at the target place are heavily affected by their mechanical and hydrodynamic properties.[14]

Drug delivery systems

The drug delivery system (DDS) is one of the most important and promising applications of polymeric nano- and micromaterials in the biomedical field. According to the National Institute of Health (NIH), a DDS is defined as a "device that enables the introduction of therapeutic substances into the body and improves efficiency and safety by the control of the rate, time and place of release of drugs in the body".[13] One of the largest research areas in the field of drug delivery is the targeted and controlled delivery of anticancer drugs.[15]

A major concern in the field of drug administration is that of being able to deliver drugs or other pharmaceutical agents to patients in the most physiologically acceptable manner. A very important principle for the use of polymer nanofibres for drug delivery is that drug particulate dissolution rates increase when the drug concentration and corresponding carrier surface area are increased.

Polymer nanofibres for controlled drug delivery are characterized by several advantages, such as, for example, a large surface area to volume ratio.[16] The possibility of delivering topical drugs opens up a number of application opportunities.

The main advantages of nanofibre-based delivery methods include the possibility of doing so in a targeted manner, thus reducing the total drug dose and, consequently, its toxicity for non-target sites, and also preventing the need for other systemic treatments, such as oral administration.[17] In drug delivery systems for biomedical application, fibres help encapsulate the therapeutic agent (Fig. 2(a and b)).[11,18,19]

To be properly controlled, drug release is usually dependent on such parameters as porosity, surface area, and degradation of polymer fibres (Fig. 2(c)). In the case of high-porosity fibres, their surface area is much larger, which is beneficial for drug release, as the number of drug-binding sites is greater.[12] The surface area and dimensions of the fibres used as cancer drug carriers are very important parameters. The very small diameter of nanofibers provides a short diffusion passage length,[20] while the large surface area is helpful in transferring the mass and effective drug release.[17] Moreover, the features of the drug

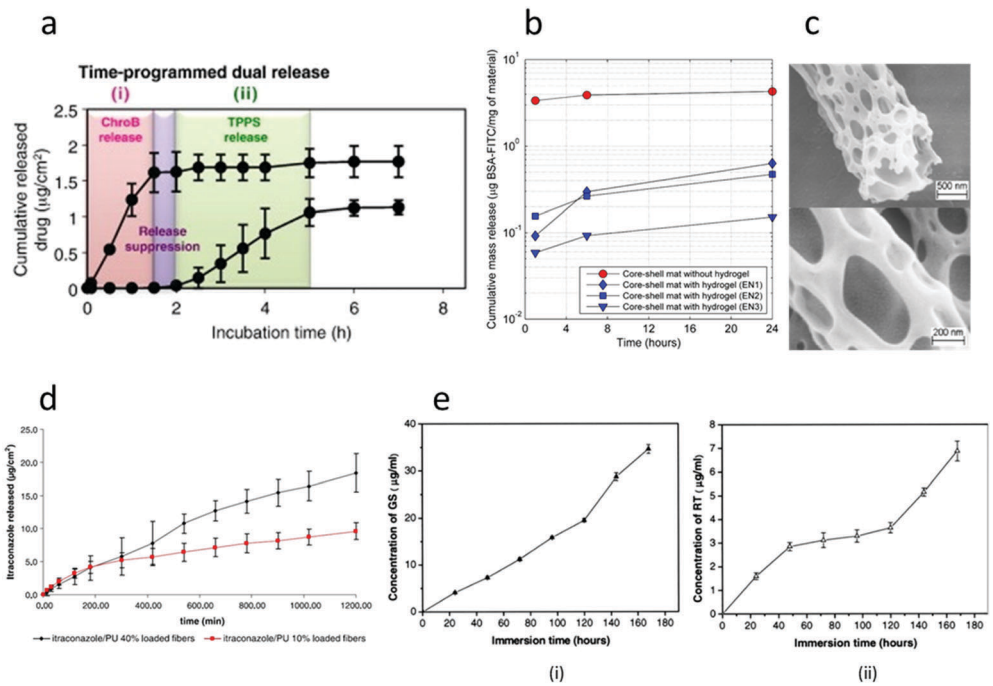

Fig. 2 *In vitro* release of drugs from electrospun fibres: (a) multilayer encapsulated therapeutic agents for slow time release; (b) release of BSA-FITC from a core–shell mat without hydrogel (red) and three different proportions of hydrogel components (blue); (c) SEM images of porous PMMA fibres; (d) release of intraconazole from polyurethane fibres; and (e) PCL with (i) 40% gentamycin sulphate (GS) and (ii) 10% resveratrol (RT) in the core. Image (a) is reprinted from Okuda *et al.*[11] with permission. Image (b) is reprinted from Nakielski *et al.*[18] with permission. Image (c) is reprinted from Dayal *et al.*[12] with permission. Image (d) is reprinted from Verreck *et al.*[17] with permission. Image (e) is reprinted from Huang *et al.*[21] with permission.

release depend on the quality of the drug encapsulation into the fibres.[16]

Drug release methods use biodegradable or non-degradable materials. These materials, which are characterized by specific features obtained by tissue engineering, release numerous drugs in a controlled way, including: antibiotics,[21,22] anticancer drugs,[15] proteins,[23,24] and DNA.[23,25] It would be desirable to succeed in designing a drug delivery device capable of releasing the desired agent in a controlled way (Fig. 2(d and e)), but that would be difficult when the material begins degrading at the time of drug release. In a biodegradable system, the drug can be released by diffusion or material degradation. In some cases, this last method leads to dose dumping, causing drug concentrations to reach toxic levels locally. This is why it is crucial to tailor the release rate and degradation rate.[26] Numerous papers on the release of drugs or dyes (as drug models) from nanofibers presented a wide range of release options (from 30% to 90% of the drug total mass). However, the release range from 80% to 90% was achieved only when the fibres were degraded during the release process.

It is worth noting that such a release process is not compatible with the theoretical predictions based on the solid-state diffusion assumption.[27] Sriker *et al.*[28] studied the release of Rhodamine 610 chloride from electrospun monolithic PMMA and PCL nanofibers, core–shell PMMA/PCL nanofibers, and PMMA/PCL blend nanofibers. The obtained results showed that in the case where there is no complete release, solid-state diffusion may not be the main mechanism. Additionally, the release rate depends on the desorption of the deposited compound from the fibre surface contacted with the water environment or from the fibre nanopores. This release rate can be manipulated by some parameters such as the nanofiber structure, and the composition and molecular weight of the polymers.

Gandhi *et al.*[29] investigated the release of bovine serum albumin (BSA) and an anti-integrin (AI) antibody, as model protein compounds, from mats of electrospun PCL nanofibers. Based on experimental research, they found that the results are consistent with a protein release kinetic dominated by the desorption from the surface of the polymer, and they proved that the PCL nanofibers are degraded only at a very low rate. Their experiments showed also that without significant degradation of PCL nanofibers, the complete release of protein contained in fibrous mats was not attained. It was found that the chemical nature of the released protein is the dominating factor which affects the enthalpy of desorption. Finally they showed that the higher amount of BSA inside the nanofibers contributed to the higher release rate of AI, therefore, the desorption of AI was facilitated by the desorption of BSA macromolecules.

Khansari and his co-workers[30] examined the release kinetics of rhodamine B (as a water soluble drug model) and vitamin B2 (as a model of drugs poorly soluble in water). These substances were released from hydrophobic and hydrophilic nanofiber mats. Fibres were monolithic: polyamide 6 (nylon 6), poly(ethylene terephthalate) (PET), poly(vinyl alcohol) (PVA), or core–shell type (based on nylon 6). For facilitating drug release control, soy proteins were used as components of nanofibers, and the release process was evaluated measuring the fluorescence intensity. The obtained results demonstrated that this process saturates at a percent release much lower than 100% release of the total embedded substance. The authors suggested that it is associated with desorption of the drug, which limits the release from nanofibers containing biopolymers. To improve the release process, the authors used poly(ethylene glycol) (PEG) as a porogen, which helped to approach 100% release of tested drugs.

Another attractive application of polymer fibre mats in surgical practice is the use of antibiotic-releasing scaffolds. Such scaffolds act as a barrier, while also controlling the delivery of antibiotics, and could potentially decrease the frequency and severity of post-surgery adhesion (*e.g.* abdominal) formations.[22]

Scaffolds for tissue engineering

Tissue engineering is an interdisciplinary field that applies the principles of life sciences and engineering for the development of biological substitutes. Its task is to maintain, restore, or improve the function of tissues and whole organs.[31] Scaffolds for tissue engineering should have several important properties, fostering oxygen and nutrient diffusion and the removal of metabolic waste during tissue regeneration. Fibre-based techniques have emerged as promising platforms for making tissue constructs, which can meet the abovementioned challenges.[32,33]

Fibre-based scaffolds ensure a support for cells to regenerate a new cellular matrix after the original one has been damaged by injury, disease, or congenital defects.[34] These materials are highly porous and behave like the extracellular matrix in the body (Fig. 3(a)).[11,35]

Nanofibres used for scaffolding must be characterized by high porosity, large surface area, uniform dimension, structural integrity with tissue, biocompatibility, biodegradability, appropriate mechanical properties, and nontoxicity for cells.[12] The four most important types of scaffolds for tissue engineering include tissue scaffolds for nerves, artificial blood vessels, cartilage, and bone tissue.[36,37]

Recent advances in nerve regeneration based on the application of the principles of tissue engineering have contributed to the development of a new perspective for nerve therapy. The success of neural tissue engineering is mostly based both on the tissue progression and on the regulation of cell behaviour through the development of a synthetic scaffold.[38] Scaffolds made of polymer nanofibres help to regenerate the damaged central nervous system. Their structure is similar to the extracellular substance of the central nervous system, and their porosity contributes to the inhibition of glial scars.[39] Such synthetic scaffolds must also be biocompatible, immunologically inert, biodegradable, and consist of infection-resistant biomaterial to support neurite outgrowth and electroconductivity.[40] Other very important properties needed for successful graft uptake by host tissues are the compatibility and mechanical stability of scaffolds. The structure of

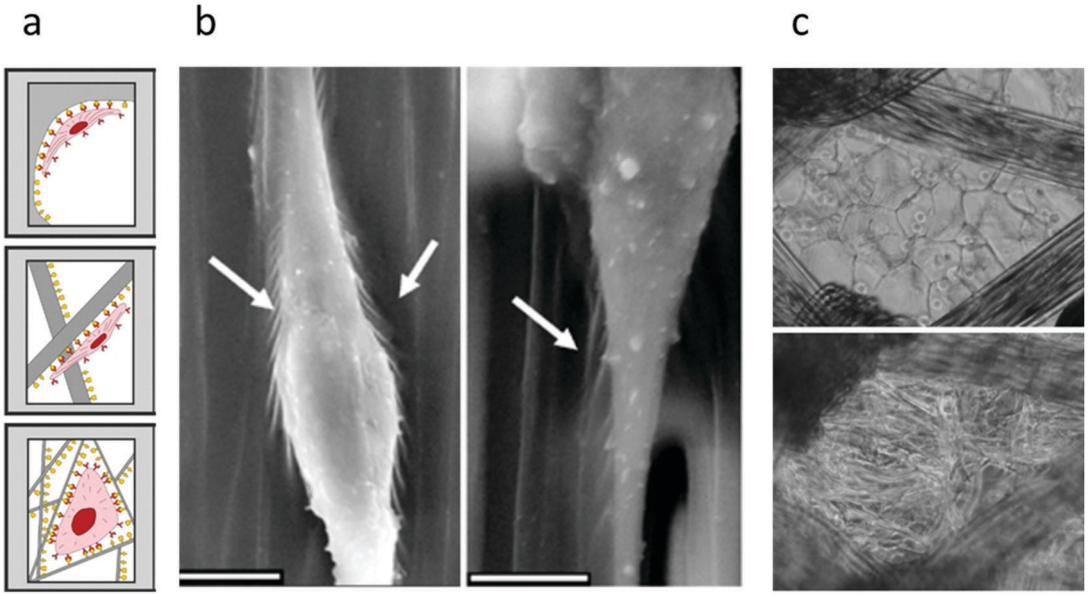

Fig. 3 Applications of polymeric fibres for tissue engineering: (a) scaffold architecture with binding and spreading of cells; (b) cell-matrix adhesion among the three different scaffolds of PLLA fibres and neural stem cells; and (c) PLGA–collagen hybrid mesh with fibroblasts after 5 days of cultivation. Image (a) is reprinted from Stevens *et al.*[35] with permission. Image (b) is reprinted from Yang *et al.*[41] with permission. Image (c) is reprinted from Chen *et al.*[46] with permission.

nanofibres influences the behaviour of cultured cells which grow according to the orientation of the nanofibres, resulting in better nerve regeneration (Fig. 3(b)).[41] There is a wide choice of polymers available with the required properties. In various nerve regeneration approaches both natural (like alginate, collagen, chitosan, chitin, and gelatin), and synthetic polymers have been used. The group of synthetic polymers includes: biodegradable polymers such as PLGA, poly(ε-caprolactone) (PCL), and poly-L-lactic acid (PLLA), non-degradable polymers (silicone), and conducting polymers (polyaniline, polypyrrole). It is preferable, however, to use biodegradable materials to prevent the chronic inflammation and compression of nerves over time.[38,42]

Another important area of nanofibrous scaffold application is the development of blood vessels. Indeed polymeric fibres are considered one of the best materials for scaffolds to be used for the formation of blood vessels. However, fibres made of natural collagen have poor mechanical properties. Those produced from biodegradable polymers (*e.g.* PGA) have better mechanical properties and high biocompatibility. PGA is easy to mould but quickly dissolves and has little resistance to cyclic pressure changes. Polyurethane foam copolymers (PHA, PLA) and polyethylene glycol (PEG) are used to minimize the shortcomings of PGA, resulting in better mechanical properties and higher biocompatibility.[43] The polymer structure of nanometric fibres is similar to the basement membrane: therefore, some attempts have been made to use polymeric membranes (PLA or PCL) with collagen-coated fibres. The results indicate that collagen coverage improves endothelial cell viability, adhesion to the substrate, and mechanical properties, while, in addition, seeded cells do not require any further growth factor stimulation.

Cellular scaffolding based on structured scaffolds is one of the most effective ways to repair damaged cartilage tissue.[44] Typically, polymers such as polylactic acid (PLA), poly-glycolic acid (PGA), or polycaprolactone (PCL) are used for this purpose. It appears that the best biomaterial used for this purpose is PCL. The scaffolds made of this substance have a high porosity and ratio of nanofibre surface area to occupied volume, and are morphologically similar to natural collagen fibres. It is also possible to produce them in any shape and size, and they are stable substrates. Scaffolds made from PLLA (poly-L-lactide), collagen, and PLGA (lactide-glycolide copolymer) have also been tested *in vitro*. It has been shown that under these conditions they are suitable for the regeneration of cartilage tissue. Their density is comparable to the density of natural tissues and they continually produce type II collagen.[45] Collagen-based porous scaffolds are commonly used for skin tissue engineering Fig. 3(c).[46] Wise *et al.*[47] worked on the creation of a tissue-like construct that can mimic the superficial parts of articular cartilages. They cultured human mesenchymal stem cells (hMSCs) on oriented fibrous electrospun polycaprolactone (PCL) scaffolds, and also on randomly porous PCL films containing a growth medium or chondrogenic differentiating media. The orientation and proliferation of cells as well as the chondrogenic marker amount were quantitatively measured. The authors found that hMSCs cultured on PCL scaffolds maintained their initial orientation even after 5 weeks. They also suggested that the creation of articular cartilage superficial parts can be significantly improved thanks to the combination of nanofibrous scaffolds and stem cells.

Attempts are also being made to develop biodegradable materials capable of becoming bone replacers. They must have the appropriate mechanical properties at each stage of bone

formation, be osteoconductive, and degrade at a certain rate, leaving room for cells to form.[43] Moreover, polymers such as PCL, PGA, PLA, or PLGA, polymer composites, and biodegradable ceramics (hydroxyapatite, calcium triphosphate, calcium carbonate) are used to produce scaffolds which are used in bone tissue culture.[48] As with the scaffolds for the development of cartilage tissue, it is important for the materials to be similar to the mineralized phase of the extracellular matrix of bone tissues. The polymer used as a matrix for ceramic particles permits the free shaping of the implant, and solves the problem of the brittleness inherent in ceramics. What is more, this composite system has better osteoconductive properties than pure polymers. Polymer nanofibres with calcium carbonate particles show much better osteoblast adhesion than polymeric nanofibres.[48]

Dynamics of nanoobjects suspended in liquid

For biomedical application, crucial is understanding of the dynamics of individual polymer objects. The behaviour of suspended micro- and nanoobjects depends mainly on their geometry and material parameters. In the case of spherical particles, their geometry is described by a single dimension, usually defined by their physical diameter. Deformable droplets or solid rods are characterized by three dimensions: height, width, and length. In addition, for droplets, the viscosity ratio characterizes their deformability in a shear flow. In the case of more complex structures, such as elongated and deformable fibres, apart from the dimensional parameters, their deformability is characterized by the fibre material elasticity. Knowledge of these parameters is essential for describing the mobility of objects suspended in a liquid.

Brownian diffusion

Thermal energy causes random movements of molecules or small particles suspended in fluids. A colloidal material suspended in a fluid kept at absolute temperature T has, on average, a kinetic energy $k_BT/2$ associated with movements along each coordinate, where k_B is the Boltzmann's constant. Such chaotic movements of particles (micro- and nanoobjects) are due to their collisions with molecules in the fluid in which they are suspended. This phenomenon was discovered by the Scottish biologist Robert Brown (1827). He observed, under a microscope, an incessant movement in random directions of pollen suspended in water. Einstein (1905) and Smoluchowski (1906) contributed with their independent work to the complete understanding of this phenomenon and determination of its mathematical description. They discovered the relationship of the chaotic pollen motion found by Brown with the thermal fluctuations of the molecules in the solvent (water). Water molecules bombarding particles of pollen initiate their random movements. This is a manifestation of the thermal energy: the temperature is a measure of the intensity of the pollen movements observed. According to Smoluchowski, this can be interpreted as stochastic fluctuations of particle density, which are responsible for diffusion processes. By observing the Brownian motion of suspended objects and evaluating their trajectories, it is possible to obtain detailed information about the environment in which the analysed objects are suspended. It is worthy of note that diffusion processes, which are relatively slow at macro scales, are the most effective mechanisms for small-scale material transport within fluids.[49]

Brownian movement is responsible for diffusion phenomena, *i.e.* the spontaneous spreading of molecules or particles in space. Depending on the scale of the phenomenon, we consider two basic types of diffusion:

(1) Molecular diffusion – this process comprises the molecular quantities of matter (or energy) usually referring to the diffusion equation, and leads to the equalization of the concentration (or temperature) of each of the diffusible substances in the whole system. This kind of process is typically described mathematically by using Fick's law of diffusion.[50]

(2) Tracer diffusion – this process relies on the microscopic chaotic motion of single particles (Brownian motion), depending on their mobility tensor.[51]

Diffusion coefficients for these two types of dispersion are generally different because the diffusion coefficient for molecular dispersal is binary and includes the effects of the movement of different diffusing species. In this work, we concentrated on the second type of the phenomenon, analysing the particle mobility to evaluate the diffusion process. A single-particle tracking method, based on optical techniques, is used to record the trajectory of a moving microparticle.[52]

Einstein and Smoluchowski concluded that the observed Brownian movement of the particles suspended in a liquid is direct proof of its molecular structure. They suggested that the study of the mobility of Brownian particles permits the detailed analysis of solvent properties. Their work proved the direct relation between the mean square displacement of the observed particles ($\langle x^2 \rangle$, MSD) and the diffusion coefficient D, which can be measured applying the following formula (eqn (1)):

$$\mathrm{MSD} = \langle (\Delta x(t))^2 \rangle = 2a_d Dt \quad (1)$$

where: $\Delta x(t) = \mathrm{abs}(x(t) - x(0))$, the particle displacement during an interval time t; a_d – the space dimension.[52] The MSD value is evaluated as a time or space average over a large number of observed displacements.

For spherical particles suspended in a homogeneous liquid, diffusion is determined by the translational diffusion coefficient and the usually neglected rotational diffusion coefficient. In the case of asymmetric particles (elongated shape objects), non-isotropic translational diffusion coefficients are possible: along the main axis (D_a) and along the minor axis (D_b). Here, also, the rotational diffusion coefficient D_θ is not negligible.[52,53]

The translational diffusion is anisotropic for non-spherical particles. For stiff elongated particles (rods, spheroids) we can distinguish six individual diffusion coefficients. Three coefficients are responsible for random particle displacements in each of the x, y, z directions (eqn (2)):

$$\mathrm{d}x(t_n) = x(t_{n+1}) - x(t_n) \quad (2)$$

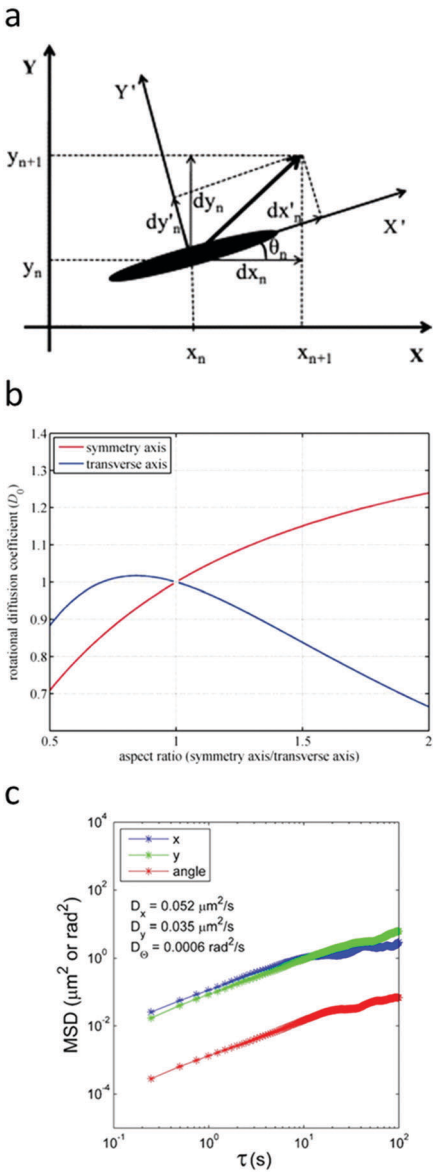

Q8 Fig. 4 Brownian analysis of micro- and nanoobjects: (a) coordination for spheroid planar rotation (X', Y' – long and short spheroid axes); (b) the rotational diffusion coefficients (referred to the symmetry axis ∥ and transverse axis ⊥) affected by ellipsoid eccentricity; and (c) the mean square displacement plot of nanofilaments as a function of lag time used for the calculation of translational and rotational diffusion coefficients (eqn (4)–(6)). Image (a) is reprinted from Charsoogh *et al.*[52] with permission. Image (b) is reprinted from Loman *et al.*[54] with permission. Image (c) is reprinted from Nakielski *et al.*[18] with permission.

and three other rotational coefficients are defined for particle rotation about each axis (eqn (3), Fig. 4(a)):

$$\mathrm{d}\theta(t_n) = \theta(t_{n+1}) - \theta(t_n) \tag{3}$$

The experimental evaluation of these complex displacements is not an easy task. Displacements in space must be observed by means of a more difficult analysis of object rotation (Fig. 4(b)). One of the methods used to determine the rotational diffusion is by evaluating static or dynamic fluorescence anisotropy.[54] By limiting observations to in-plane displacements, rotational motions are analysed only for the axis perpendicular to this plane.

The theoretical evaluation of drag forces for ellipsoidal objects moving in viscous liquid makes it possible to calculate the corresponding diffusion coefficients of long, thin ellipsoids.[49] Using such an approximation, three basic diffusion parameters of rods can be evaluated according to the following formulas (eqn (4)–(6), Fig. 4(c)):

$$D_\mathrm{a} = \frac{k_\mathrm{B}T\left[\ln\left(\frac{L}{R}\right) - 0.5\right]}{2\pi\eta L} \tag{4}$$

$$D_\mathrm{b} = \frac{k_\mathrm{B}T\left[\ln\left(\frac{L}{R}\right) - 0.5\right]}{4\pi\eta L} \tag{5}$$

$$D_\theta = \frac{3k_\mathrm{B}T\left[\ln\left(\frac{L}{R}\right) - 0.5\right]}{\pi\eta L^3} \tag{6}$$

where: D_a and D_b denote translational diffusion coefficients along and perpendicular to the rod main axis; D_θ is the rotational diffusion perpendicular to the main axis of the rod; L and R denote the length and radius of the rod ($L \gg R$); and η is the dynamic viscosity of surrounding media.

The problems of characterizing the diffusion of flexible objects, such as nanofilaments or long molecular chains, can be solved only on a statistical basis due to the large number of degrees of freedom. There are not just translational and rotational motions of the object to be analysed. The main response of thermal fluctuations is transformed into the multifunctional shape variation of the object analysed. There is no unique method for characterizing the diffusivity of such objects. The diffusivity of flexible objects depends not only on their geometry and shape, but also on a large number of parameters characterizing the constraints of internal and external mechanical interactions. Hence, it is necessary to introduce several simplifications. In the most common approach, proposed by Kratky and Porod, the complex shape variations of such an object are described in the reduced formulation as a chain of spherical subunits.[55] Its dynamic structure may be regarded as a stochastic behaviour of randomly moving chain elements connected by flexible springs. The statistics of chain deformations can be described by the persistence length, being a measure of the chain stiffness or flexibility; the stiffer the chain, the larger the persistence length.[56] As will be shown in the next section, such an approach permits a relatively straightforward interpretation of the observed shape variations in terms of basic mechanical parameters.

Mobility of nanoobjects in a flow

Predicting the behaviour of deformable objects carried by a flowing fluid is necessary for a full understanding of the physics of macromolecules, bioliquids, and filament

suspensions. The investigation of the nature of polymer nanomaterial flexibility is essential for determining their structure and dynamics, and is crucial especially in the case of materials used for targeted drug delivery and tissue engineering. Additionally, it is assumed that by investigating the dynamics of elastic objects suspended in a liquid it is possible to gain knowledge on the role of the mechanical properties responsible for the complex behaviour of biological molecules (*e.g.* the folding of DNA). Theoretical assumptions, especially in the field of polymer physics, use coarse-grained models to study the folding process of DNA. However, to describe this phenomenon on a molecular scale, such an analysis must still be limited to very small length and time scales.

The transport properties of elongated and deformable objects suspended in liquids are still far from being completely understood. Despite recent progress in this field, there is still a paucity of experimental investigations for the validation of the assumptions of numerous theoretical and numerical models. The mathematical description of mobility for stiff objects is already characterized by several serious limitations, being generally based on their shape simplifications. The simplest models of rod-like shaped particles are based on elongated ellipsoids (Fig. 4(a)), or chains of interconnected spheres (Fig. 6(c)), which are easier to accommodate to a Stokesian set of equations. Even for such relatively simple geometry, however, only the general description of their mobility properties is validated experimentally. In the case of flexible objects – mainly investigated as elements of polymer science – the details of mobility for individual molecular chains are deduced only from the available statistically averaged bulk flow data. The lack of experimental studies is mainly due to the absence of good physical models that can make it possible to determine and control the elasticity and geometry of the objects analysed.

Studies on the dynamics of flexible polymers in a flow are of central importance in materials science, mechanical engineering, biology, and medicine. In their work, Le Duc and coworkers presented observations on the real-time dynamics of individual, flexible polymers under a shear flow.[57] The experimental results of these authors showed that conventional approaches, such as birefringence and light scattering, which measure only ensemble-averaged molecular parameters, overlook the extremely rich dynamics of individual polymers under shear. Their observations also provide an insight into the conformational and orientational changes of polymers in a shear flow, and a basis for further theoretical modelling.[58]

One of the most interesting behaviours of nano- and microobjects suspended in a liquid is their cross-flow migration. This is a phenomenon involving the movement of the examined object across the width of the channel in which it was placed, under the influence of forces associated with the flow. This effect has a long history of research, initiated by the intriguing redistribution of red blood cells in capillaries (Fig. 5(a)) observed by the pathologist Fåhræus.[59,60] Some early experiments conducted by Segre and Silberberg[61] on spherical particles observed in a tube flow confirmed the existence of lateral hydrodynamic forces which redistribute the suspended particles across the channel to the equilibrium position between the tube wall and its centre. As a solid particle is obviously a very coarse approximation of highly deformable blood cells, liquid droplets suspended in the flow were used as models of erythrocytes.[62] These preliminary studies indicated the presence of cross-flow migration and paved the way for a chain of studies devoted to elucidating the role of shear stresses, wall interactions, droplet deformability, and viscosity ratios in the migration process.[63–66] One of the important messages originating from these studies is that the inertial forces, usually neglected in microfluidics, play an important role for the proper interpretation of the cross-flow migration of particles and droplets.[67] The presence of residual inertial forces and the breakup of the flow symmetry in the case of suspended deformable objects lead to irreversible hydrodynamics, imposing a limited use of the so-called Stokesian approximation of theoretical models. This became evident in microfluidic experiments on the lateral migration of droplets.[68,69]

In 1956, Starkey[70] was the first to demonstrate that – under appropriate conditions – neutrally rigid spheres in Poiseuille flow could migrate across streamlines. Very interestingly, many studies observed that these spheres eventually attained an equilibrium position at approximately 0.6 of the tube radius from the tube centre. Segre and Silberberg called it the ''tubular pinch effect''.[61] This effect was confirmed in the following years by other researchers.[71,72]

Suspension behaviour is one of the fundamental challenges of modern rheology.[73,74] There are numerous experimental reports on the migration of solid particles[61,75] and droplets (Fig. 5(b and c)).[64,76] They confirm the presence of radial migration, but the theoretical interpretation of this phenomenon is still a subject of controversy. Ho and Leal presented the lateral migration velocity of particles in a two-dimensional Poiseuille flow.[77] The main outcome of the model is that there is, in fact, effective cross-flow migration, even for the low, but finite, Reynolds number flow regime. For deformable objects the most impactful work by Chan and Leal showed that deformable droplets migrate across the flow streamlines.[63] Their research proved that even in the creeping flow regime the particle (droplet) deformation creates the conditions for irreversible cross-flow migration. A recent study, focusing on the use of an oscillatory flow, indicated that cross-flow migrating droplets follow some complex spiral-like paths with parameters additionally depending on the frequency and phase lag of the imposed flow (Fig. 5(b)).[69] The migration may change direction depending on the viscosity ratio, while droplets can migrate either into the flow axis or to the channel wall. To some extent, elongated viscous liquid threads could be treated as a model configuration of polymer filaments. However, as we find in the following section, their mechanical properties are quite different.

The cross-flow migration problem is complex in the case of elongated objects. In most cases, microscale migration effects of elongated objects are simplified to an ellipsoidal model introduced by Jeffrey,[78,79] and possibly applied to stiff fibres. Most of the theoretical models describing the behaviour of

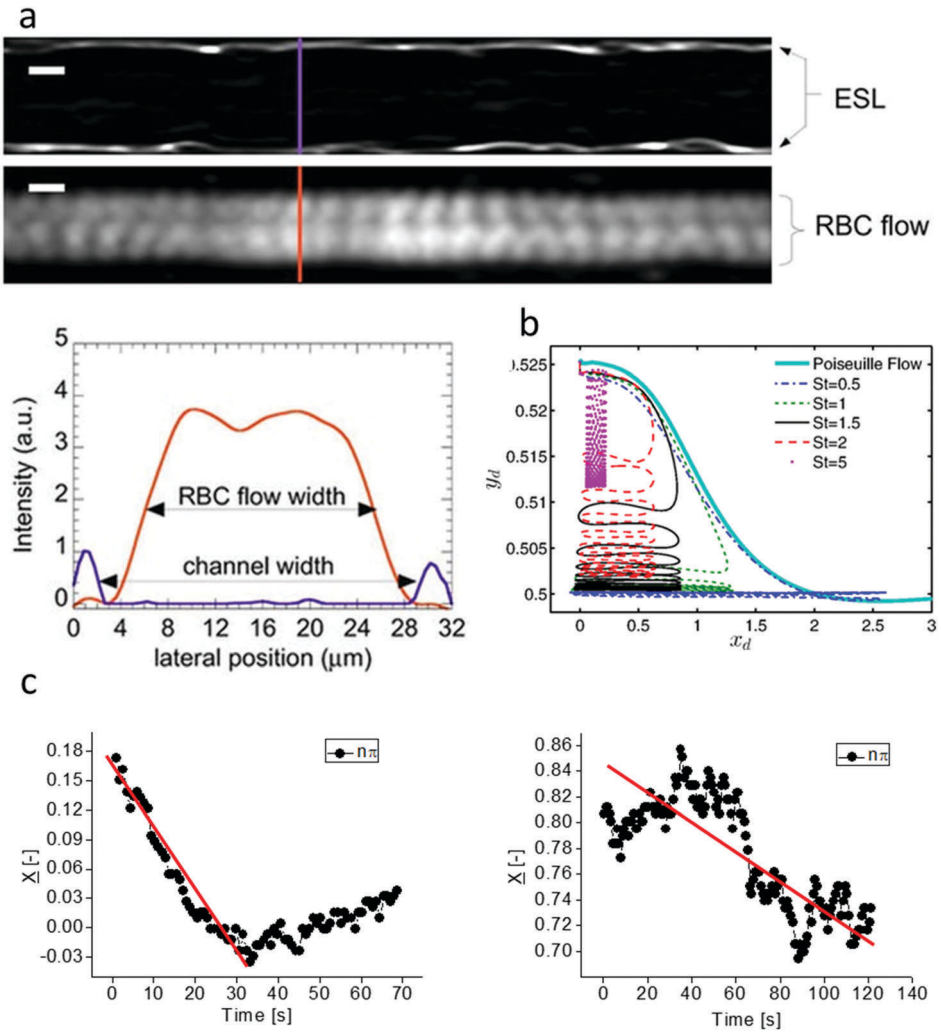

Fig. 5 Cross-flow migration of spherical microobjects: (a) scheme of the position of the Endothelial Surface Layer (ESL) at the walls and the Red Blood Cells (RBC) in the centre during the flow, scale bar: 10 μm; (b) trajectory of a droplet in different flow conditions represented by the spiral-like path of a droplet under the influence of oscillatory flow (droplet position in the channel: y_d – width and x_d – length); (c) cross-flow migration of 1 μm polystyrene particles under an oscillatory flow with different initial positions from the centre of the microchannel as a function of time, $\underline{x}$ – relative distance (distance from the channel centre), [0,1] denotes the microchannel centre and the wall, respectively. Image (a) is reprinted from Tsvirkun *et al.*[60] with permission. Image (b) is reprinted from Chaudhury *et al.*[69] with permission. Image (c) is reprinted from Pawłowska *et al.*[75] with permission.

particles in a microflow are based on the reversible, creeping flow approximation. Creeping (Stokesian) flow models, however, can be misleading in the case of deformable objects and complex flow structures. Thus, despite the widespread belief in creeping flow reversibility, irreversible hydrodynamics are commonly present for deformable objects and in curved microchannels.[80] Therefore, we may expect irreversible hydrodynamic interactions even for the creeping flow of flexible filaments observed in a microchannel. One of the most common effects of such interactions is the cross-flow lift force exerted on suspended objects, which is due to the wall and velocity profile interactions and depends on a number of factors. Depending on the geometry ratio, physical properties of suspended objects, and degree of shape deformation, the cross-flow migration may lead to the uneven distribution of suspended objects across the channel, and their consequent collection at one or more equilibrium radial positions (Fig. 6(a)).[62,63,65,81] The migration problem is quite complex in the case of long flexible objects (*e.g.* filaments, molecules). Without a doubt, this phenomenon is affected by changes in conformation, object elongation, or tumbling.

The cross-flow migration of fibres or other long objects in a channel flow is one of the fundamental issues of modern lab-on-chip techniques, being important in a variety of biological, medical, and industrial contexts (*e.g.* Brownian dynamics of DNA or biological polymers, cell movement, movement of microbes, and drug delivery). The microfluidic systems developed for focusing and sorting cells and biological objects are based on the hydrodynamic interactions responsible for the cross-flow migration of selected objects suspended in the carrier liquid. The existing simulations conducted for long objects suspended in a flow suggest that stiff fibres tend to

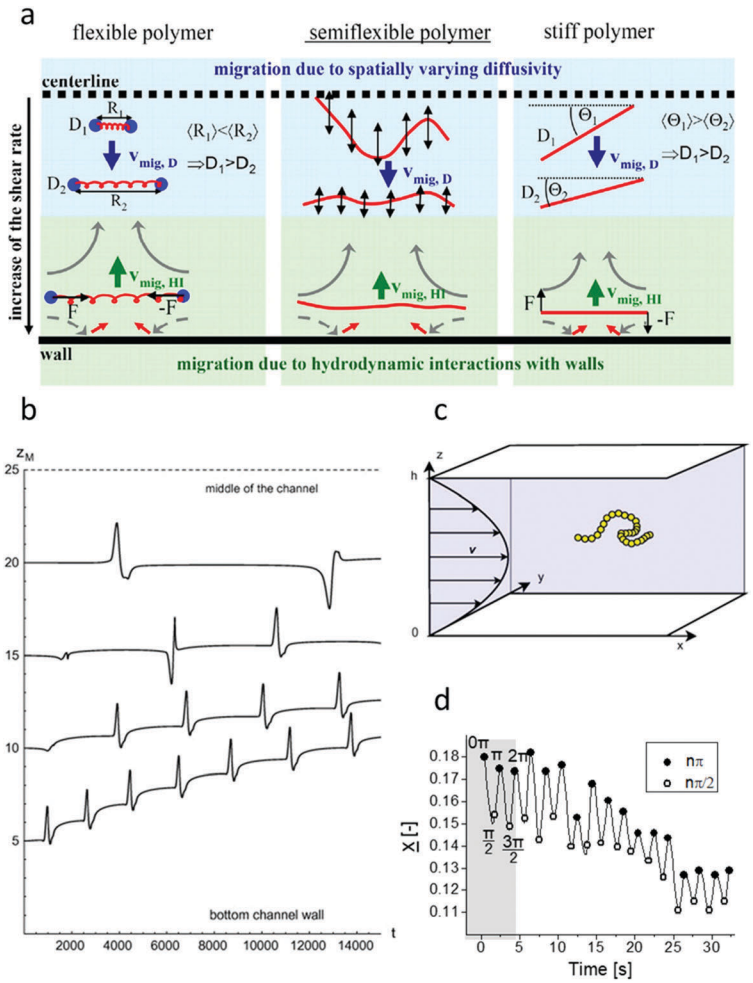

Fig. 6 Cross-flow migration of elongated micro and nanoobjects: (a) migration and changing of conformation and orientation of polymer chains characterized by different flexibility; (b) fibre centre of mass migration trajectories from different initial distance from the centreline of a microchannel as a function of time, described by the "flexible fibre model" (schematically shown in (c)); (c) model of a chain of beads under the influence of Poiseuille flow inside a microchannel; and (d) changing of position of a hydrogel nanofilament across the microchannel width during an oscillatory flow ($\underline{x}$ – relative distance from the channel centre). Image (a) is reprinted from Steinhauser[81] with permission. Image (b) and (c) are reprinted from Sadlej *et al.*[76] with permission. Image (d) is reprinted from Pawłowska *et al.*[75] with permission.

accumulate near the channel wall, while flexible fibres undergo great deformations and accumulate far from the wall (Fig. 6(b and c)).[74,76] Long filaments have the tendency to accumulate near the wall and bend only slightly.[73,76] On the other hand, the flexible fibres conveyed by the flow tend to accumulate rather far from the wall, where they bend significantly.[74] A detailed experimental validation is still unavailable for such data.

Q10 Other studies on the self-organization of semi-flexible long objects along the channel cross-section depending on different flow velocities show the tendency of fibres to elongate or bend in a microflow. The fibre elongation increases as the flow rate increases. In addition, the flow rate also affects the equilibrium position of fibres across the channel. At a high flow speed, there is little chance of finding fibres near the centre of the channel. Fibres may migrate from the centre of the channel to the walls, and modify the shear rate of the flow near the wall.[81] Such an effect is known for polymers used to damp the development of the turbulent boundary layer at a channel wall.[82]

In our recent paper we presented the results of an analysis on flexible hydrogel nanofilament cross-flow migration (Fig. 6(d)).[75] We showed that one of the most important parameters affecting the lateral migration and diffusivity of long polymers is the filament conformation.

For this reason we selected three groups of nanofilaments (bent-like, U-shaped stretched, and U-shaped buckled filaments), characterized by different behaviours and directions of lateral migration during the flow. The aim of this investigation was to evaluate how the contour length of a nanofilament and its shape determine the cross-flow migration inside the microchannel. The distribution of the centre-of-mass position for bent and U-shaped hydrogels was observed over time. We observed that, in the presence of an oscillatory flow, the nanofilament distribution shifts closer to the centreline of the microchannel in the case of bent nanofilaments, and further away for the U-shaped stretched nanofilaments. The tendency of the chain to equilibrate its conformation in the

presence of hydrodynamic forces determines the cross-flow migration. In the case of hydrogel nanofilaments, this depends both on the magnitude of the flow applied and on their initial shape.

Mechanical properties of elongated particles

The knowledge of the mechanical properties of polymers is important in the context of their applications (*e.g.* medicine, industry). It is especially important that they have suitable strength, stiffness, and toughness. For the correct determination of their mechanical properties, it is crucial to understand the relationships among molecular structure, morphology of the materials, and their final mechanical properties. The strength reveals the material resistance to damage caused by breakage or excessive deformation, while stiffness is a measure of the load required to cause a deformation in the material. Stiffness is determined by measuring the deformation resulting from the application of a given load (force), which does not damage the object. Stiffness is the rigidity of an object; it carries shape information of the sample. A complementary definition of stiffness is material flexibility; the more flexible an object is, the less stiff it is ref. 83 and 84. As we showed in our paper, the stiffness of elongated nanoobjects affects their mobility.[18] We observed that a filament straight shape and greater stiffness are correlated with relatively high longitudinal diffusion (Fig. 7(a)). For this reason, it is necessary to include shape parameterisation in order to find any possible correlation between stiffness and diffusion.

A common method for determining the stiffness of polymers is the use of the persistence length (L_p) value. The persistence length refers to the ability of the sample to independently deform under the influence of thermal fluctuations when its segments are at distances above L_p. Generally speaking, the pieces of polymers that are shorter than their persistence length behave like flexible elastic rods, while the deformability of the pieces of polymers that are much longer than their persistence length can only be described statistically as a three-dimensional shape fluctuation. In other words, the persistence length is the length after which the polymer chain loses its initial orientation.[85] The value of L_p varies from 0 to ∞. Bending rigidity – a fundamental parameter used to describe the conformation of long polymeric objects – is related to persistence length. It determines the object bending deformation due to the external forces applied.[85]

The first model defining persistence length for molecular chains was offered by Bressler and Frenkel.[86] Ten years later Kratky and Porod evaluated it in the better-known form of a worm-like chain of small segments.[55] They proposed that the bending potential $U(\theta)$ of the elastic rod (contour length L) which bends at an angle θ in the first approximation must be

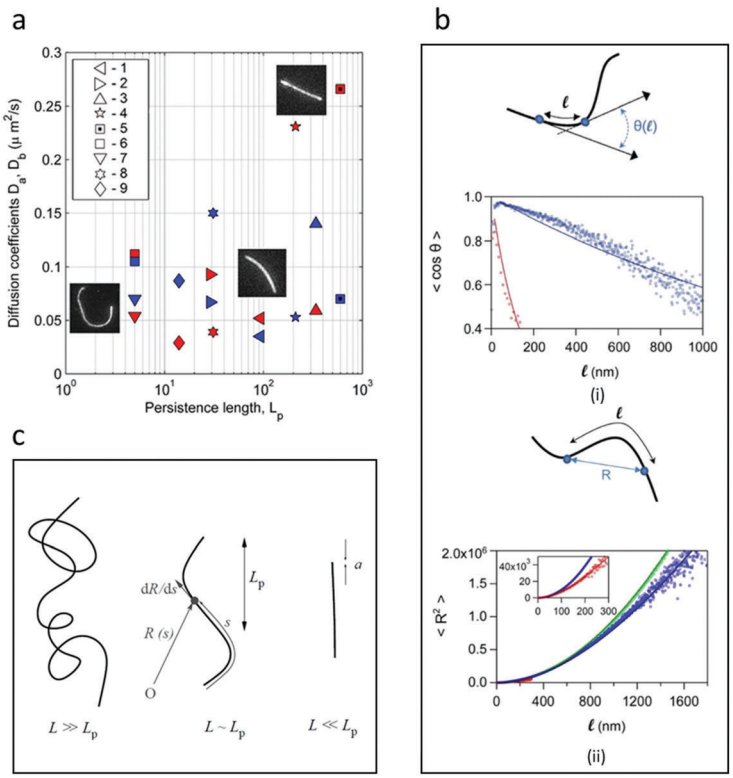

Fig. 7 Mechanical property analysis: (a) influence of mechanical properties (stiffness) of fibres on their mobility (numbers 1–9 represent individual fibres with different contour length and shape); (b) persistence length evaluation methods (ℓ – distance along the chain contour between two designated points on this contour; red, blue, and green circles represent data for three different amyloid fibrils): (i) cosine correlation and (ii) end-to-end distance R analysis; and (c) stiffness of elongated micro- and nanoobjects, described as a ratio of contour length to persistence length. Image (a) is reprinted from Nakielski *et al.*[18] with permission. Image (b) is reprinted from Lamour *et al.*[90] with permission. Image (c) is reprinted from Liverpool[89] with permission.

proportional to the square of that angle. With an increased contour length of the rod, its bending potential decreases. The effective parameter determining the deformability of the molecular chain is the ratio of the persistence length (L_p) to the contour length (L).[87] This parameter is called relative stiffness (b_s) (eqn (7)):

$$b_s = \frac{L_p}{L} \tag{7}$$

There are three methods commonly used to evaluate the persistence length (Fig. 7(b)):

(1) Cosine correlation – this method is based on the analysis of the two-dimensional cosine correlation of the tangent angle (θ) along segments (s) of the long object with a contour length L. It uses the fitting function (eqn (8)):

$$\cos\theta(s) = \langle\cos[\theta(s) - \theta(0)]\rangle = e^{-L/2L_p} \tag{8}$$

where $\theta(0)$ is an initial reference angle. The symmetry of the cosine function ($\pm\theta(s) - \theta(0)$) is not convenient for fitting it to experimental data. Thus, for the evaluation of the persistence length, data are fitted to an exponential function.[85,88–90]

(2) End-to-end distance analysis – this method uses the mean square of the end-to-end distance ($\langle {R_n}^2\rangle$) as a function of the contour length (L) and persistence length (eqn (9)):

$$\langle {R_n}^2\rangle = 2{L_p}^2\left(e^{-L/L_p} - 1 + L/L_p\right) \tag{9}$$

It permits the direct determination of the persistence length, but it is less accurate than the cosine correlation method. Each object is represented as a single data point, so this method shows the global geometry of an individual object. Therefore, from a statistical standpoint, it requires the analysis of a large number of samples.[85,90,91]

(3) Bending mode analysis – this method is used to analyse the shape fluctuations of single elongated objects.[88] It determines object angular bending modes through the Fourier analysis of the object shape. The persistence length is calculated using the amplitude of several bending modes and taking their weighted average. The method was found particularly useful for analysing the flexural stiffness of the microtubules responsible for driving the mitosis of eukaryotic cells.[91,92] There, a single microtubule fixed at one end changes its shape due to the thermal fluctuations damped by the hydrodynamic drag. Usually, the contribution of up to ten bending modes is necessary to estimate the microtubule flexural rigidity.

Short filaments characterized by low relative stiffness behave – in terms of conformations – in the same way as long, very stiff molecules. If the value of the relative stiffness b_s is below 0.05, the material is treated as a flexible object ($L \gg L_p$).

The object may be considered as a system of freely connected segments (*e.g.* long DNA fragments). If the value of b_s is in the range $0.05 < b_s < 5$, the filament is characterized by a reduced stiffness (semi-flexible, since $L \cong L_p$). Actin filaments are examples of semi-flexible biomolecule structures.[81] Molecules with a relative stiffness higher than 5 are identified as rigid and non-deformable ($L \ll L_p$) (Fig. 7(c)).

Physically speaking, the persistence length of nanofilaments may be described as the ratio of the bending rigidity (κ) and thermal energy (k_BT). Bending rigidity depends on the Young's modulus E and also on the moment of inertia (I) based on the filament cross-section[93,94] (eqn (10)):

$$L_p = \frac{\kappa}{k_BT} = \frac{EI}{k_BT} \tag{10}$$

where $I = \pi R^4/4$. T is the absolute temperature, k_B is the Boltzmann's constant, and R is the radius of the filament. This relation can be used to evaluate the mechanical properties of nanofilaments.

Shape fluctuations of a flexible filament suspended in a viscous liquid are damped according to the Stokes law. Assuming that the persistence length represents an elementary unit of such a flexible chain, we may define the flexural diffusivity D_f (eqn (11)), which represents the ratio of kinetic thermal energy of the environment k_BT to the Stokesian drag exercised on the "free" fragment of the chain represented by its persistence length L_p (*cf.* Table 4.2 ref. 95):

$$D_f = \frac{k_BT}{8\pi\eta L_p} \tag{11}$$

Method for nanofilament fabrication

Nanofibres are unique nanostructures with extraordinary potential in both technical and medical areas. Filter applications, functional textiles, fibre reinforcement, drug delivery, wound healing, and tissue engineering are just a few examples of their potential applications. The term nanofibre commonly applies to a fibre with a diameter of less than one micrometre. The manufacture of objects characterized by such a small size requires the use of special techniques. Electrospun and solution blow spun nanofiber mats are the most frequently used polymeric materials for developing platforms with potential biomedical applications. They were successfully loaded with different drugs, molecular markers and nanoparticles as it was presented in one of the previous sections.

Electrospinning method

The electrospinning (ES) method is a process that forms nanofibres through an electrically charged jet of polymer solution or polymer melt. This technique provides a simple and versatile method for producing ultrathin fibres from a wide range of materials that include polymers, composites, and ceramics. Electrospun fibre diameters usually range from tens of nanometres to a few micrometres.[96,97] The electrospinning of polymers was invented by Formalas[98] in 1934. He described an apparatus using electrostatic forces to draw down polymer solutions. However, it took over 50 years until the method was rediscovered for the production of nanofibres.[99]

The basic setup for electrospinning consists of three major components: a high-voltage power supply (usually in the range of 1 to 30 kV), a nozzle (a metal needle), and a collector (a grounded conductor). The nozzle is connected to a syringe filled with a polymer solution. When a high voltage is applied,

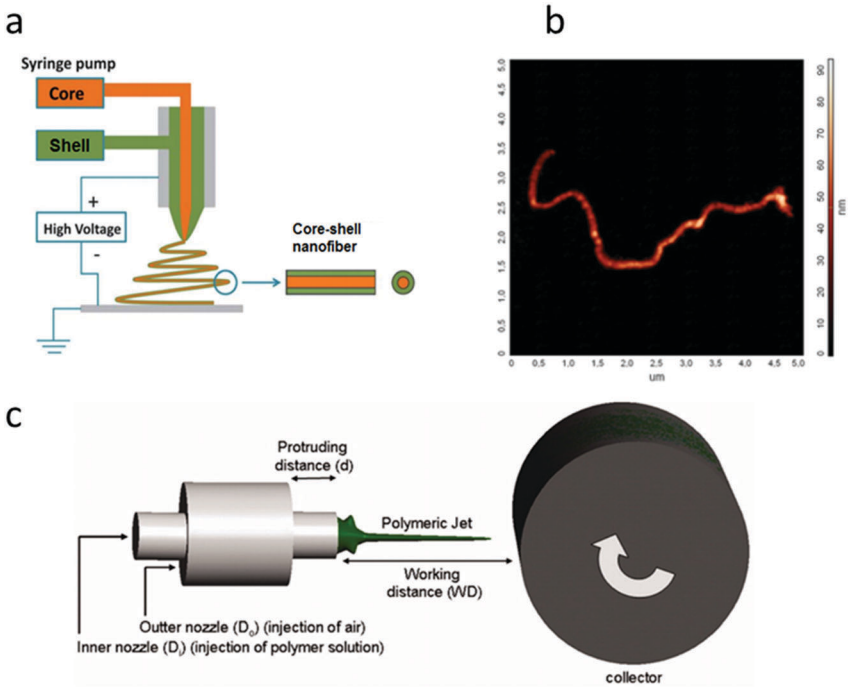

Fig. 8 Schematic of fibre fabrication processes: (a) the co-axial electrospinning method; (b) a (poly-isopropylacrylamide-*N*,*N*′-methylene bisacrylamide (PNIPAAm-BIS-AAm)) hydrogel nanofilament fabricated using the co-axial electrospinning technique (AFM topography); and (c) scheme of the solution blow spinning process. Image (a) is reprinted from Qu *et al.*[111] with permission. Image (b) is reprinted from Nakielski *et al.*[18] with permission. Image (c) is reprinted from Oliveira *et al.*[120] with permission.

the pendent drop of the polymer solution at the nozzle becomes highly electrified and the induced charges are evenly distributed over the surface (Fig. 8(a)).[18,100,101] Lastly, the drop is subjected to two major types of electrostatic forces: the electrostatic repulsion between the surface charges, and the coulombic force exerted *via* the external electric field. Under the influence of these electrostatic interactions, the liquid drop is distorted into a conical object, generally known as the Taylor cone.[100–103] As the liquid jet is continuously drawn out and the solvent evaporates, its diameter becomes significantly reduced from hundreds of micrometres to tens of nanometres. Being attracted by the grounded collector placed under the pipette, the charged fibres are often deposited as a nonwoven mat.[100] The collector has a significant impact on the arrangement and productivity of nanofibres and their final structure. This is due to its effect on the ability of the charges on fibres to be brought to ground which, in turn, affects the amount of fibres that are collected on the substrate.[104] The collector orientation influences the fibre alignment. Different collector models also affect the properties and morphology of the nanofibres produced.[105] There are several different collectors used to produce aligned nanofibres in electrospinning experiments: plane plate collector, drum rotatory collector, grid type collector, *etc.*[106] The surface area can be increased to enable the faster evaporation of residual solvent molecules by using a porous collector plate. Compared to a non-porous collector plate, the porous collector yields fibres with lower packing density. A rotating collector is useful in obtaining dry fibres as it ensures more time to let the solvent evaporate.[105] Electrospinning combined with blow spinning is considered the most promising technique for scaling to commercial production.[96]

There are a number of applications for electrospun polymer fibres and nonwovens: filters, smart textiles, protective clothing, templates, catalysis processes, sensors, functional materials, composite reinforcements, cosmetics, and also in medicine (tissue engineering, transport and release of drugs, cancer treatment, wound healing, artificial blood vessels, inhalation therapy) and electronics (batteries/cells and capacitors).[96,97,100–102,107,108]

Electrospinning permits mixing or encapsulating different components of spun material. One of such methods offers a core–shell system with a special co-axial nozzle. The nozzle consists of two co-axial cylinders (*e.g.* needles) supplied with two different solutions. As in the conventional electrospinning process, the two-component jet is simultaneously pulled, stretched, elongated, and bent *via* electric forces.[109,110] During core–shell electrospinning, two different solutions are dosed at the same time through the inner and outer needles, and are charged in the same way as in the classic single nozzle. The resulting core–shell fibre consists of two material structures in which one is surrounded by the other (Fig. 8(b)).[18] The coaxial electrospinning depends on the same parameters as those in conventional electrospinning.[111–114] Using precisely controlled syringe pumps, the flow rate of each component can be varied to control the dimensions of the core and shell material,[109,110] as well as the overall nanofibre diameter.[115] For the proper encapsulation of the core material, the flow rates of both components should be carefully matched. If the core-to-shell flow rate ratio is too low, an insufficient outflow of core

solution cannot ensure a continuous smooth core phase, and only a chain of small droplets is encapsulated.[111]

Q12 One of the best advantages of the core–shell technique is the effective protection of biological agents which are easily denatured, and the potential to enclose all substances within the core, regardless of polymer–drug interactions. Thanks to this behaviour it is possible to incorporate drugs, proteins, and even genes into nanofibres, by dissolving them in the core solutions.[21]

Solution blow spinning process

The solution blow spinning process (SBS) is a relatively new method for the production of nanofibres which is characterized by a high throughput.[116,117] It is used to fabricate polymer micro- and nanofibres with a rich variety of diameters, ranging from a few tens of nanometres to several micrometres. SBS can be applied as solution or melt spinning, and combined with electrospinning. The fibres produced by SBS are at least one or two orders of magnitude smaller in diameter than those produced by conventional fibre production methods (*e.g.* the melt spinning process).[118] Solution blow spinning makes possible mass production of nanofibres.[96,119] SBS is based on the high speed of decompressed air leading to rapid stretching and on the solvent evaporation of a jet of polymeric solution issued from concentric nozzles in the system outlet. The high-pressure air applied permits solution blow spinning to be easily scaled-up.[120,121]

The main component of the solution blow spinning apparatus is a system of specifically designed concentric nozzles. The polymer solution is supplied through the inner nozzle of this system *via* a syringe pump with a controlled injection rate, while compressed gas (*e.g.* air, nitrogen, argon) is supplied through the outer nozzle. Fine polymer nanofibres are collected on a rotating drum (collector). The collector is positioned at a fixed working distance from the nozzle. The geometry of the nozzles generates a region of low pressure around the inner nozzle which helps draw the polymer solution into a cone. Polymer nanofibres are dragged from the cone by the viscous forces of the flowing air which overcome surface tension forces (Fig. 8(d)).[96,120,121]

The solution blow spinning process is applied for the commercial production of non-woven polymer webs.[96] Due to the very small fibre diameter, a non-woven web has a high porosity and a large surface area. Such properties increase the commercial value of these materials for applications in membrane tissue engineering, scaffolds and sensors.[116,119,122]

Melt blowing is a special form of the melt spinning process which forms very fine but weak fibres.[123] It involves extruding molten polymers through a narrow orifice and into a stream of high-velocity hot air.[124] The flow of the hot air on the polymer melt surface causes the polymer to start to elongate into a fibre. This process can be controlled to produce fibres ranging in diameter from 1 μm to 50 μm (Fig. 8(e)).[96,120] These micrometre fibres are finding applications in a growing number of fields, such as absorbency, filtration, hygiene, and clothing.[124]

Methods of fibre cutting

Nanofibrous materials are usually fabricated in the form of mats,[36,39] which can be subsequently cut to form short filaments. A method to cut fibre mats has been developed by Verreck *et al.*[125] After the spinning process, the non-woven spun fabric was milled for 10 min using a cryogenic mill. Liquid nitrogen was used during the milling process for cooling the fabric and the average fibre length after milling was around 27 μm. Thieme *et al.*[126] also used the mechanical cutting of an electrospun fibre mat by cooling it with liquid nitrogen until solidification. Fibres were separated from the cutting medium by centrifugation. Ultrasonication methods are also effective for cutting fibrous membranes into short polymer filaments.[127] Duan and co-workers[128] used a razor blade at a rotation of 5000 rpm for 45 seconds in 350 ml of dioxane for cutting nanofibres into short fibres of a length of 150 ± 30 μm. The length of the fibres was controlled by the volume of the short fibre dispersion and dioxane.

One of the most interesting techniques of fibre breaking is a top-down approach developed by Castro *et al.*[129] In this method, nanoobjects (like nanofibers) were obtained by breaking down bulk materials gradually into smaller sizes. The authors used this approach to process electrospun poly(L-lactic acid) (PLLA) fibres, to obtain micro-cylinders and then an aminolysis-based chemical scission procedure was carried out. The microcylinder length was controlled by the duration of the aminolysis reaction. Porous micro-cylinders and smooth microcylinders had a length of 14.6 ± 5.77 μm and 6.6 ± 3.24 μm after 3 hours of aminolysis, respectively, but after 5 hours of aminolysis these two types of cylinders had a length of 6.6 ± 3.57 μm and 1.1 ± 0.19 μm, respectively. Aminolysis comprises a reaction between a reactive species and an amine or ammonia group donor, which causes chemical scission of the reactive species and the incorporation of amide or amine groups into its molecular structure. Also, Jing with co-workers[130] used a similar approach for preparing ultraporous fibrous polymer spongy gels by filling macroporous ultralight polymer sponges with non-wetting and wetting liquids.

Another interesting method for producing short electrospun fibres is based on the application of an electric spark. Fathona and Yabuki[131] used a polymer solution of cellulose acetate for the electrospinning process, then fibres, before falling down on the collector, passed through the gap between the tips of two electrodes that generated an electric spark. The average diameter and length of the prepared short fibres were 1 μm and 230 μm, respectively.

DNA nanostructures for drug delivery applications

In addition to artificial polymers, also natural polymers can be used for the development of fibrous materials for biomedical applications. One of the most popular approaches developed in the last few years is based on the use of DNA molecules. DNA-based nanostructures are unique platforms with high delivery possibilities and can work as nanoscale drug carriers. Indeed experimental investigations have shown that these systems exhibit great potential to achieve the ultimate goal of drug delivery, reaching maximal efficacy with minimal toxicity, moreover, DNA as a natural material is inherently biocompatible.[132,133] DNA nanoscale structures open numerous attractive possibilities to

develop new therapeutic methods, moreover, a few functionalities of such molecular devices can be triggered by cell activities in the biological environment. Numerous researches confirmed that DNA nanostructures can serve as smart drug delivery vehicles and perform complex tasks in cells.[134]

Understanding the interaction mechanism between DNA nanotubes and drugs is important for the successful development of these systems. Liang *et al.*[135] became interested in this issue and they used molecular dynamics simulation to investigate the interactions between anti-cancer drugs (doxorubicin (DOX), daunorubicin (ADR), taxol (TAX) and vinblastine (VIN)) and DNA nanotubes. The results of this simulation additionally show that the absorption of anti-cancer drugs can even improve the stability of DNA nanotubes.

Rahbani with his co-workers[136] studied DNA nanotubes functionalized (inside the tube) with lipid-like polymers as drug delivery platforms. Such structures can encapsulate small molecules and conditionally release them when specific DNA strands are added, moreover, DNA nanotubes and polymers can be connected directly and indirectly (by using spacers). A simple DNA spacer (*e.g.* thymidine) allows an intramolecular ''handshake'' to be performed, when the hydrophobic chains intermolecularly interact inside the nanotube or cage cavities. The created hydrophobic environments within the DNA cages are very useful for selective drug delivery applications. In the case when the hydrophobic chains are incapable of meeting inside the DNA structure, intermolecular association of DNA nanostructures into networks occurs. Authors suggested that introduction of orthogonal hydrophobic interactions into DNA nanotubes can significantly affect their self-assembly, ability for encapsulation, intracellular behaviour and cell uptake.

DNA bundles in a structure of multihelices could increase the nanomaterial functionality and be used as model architectures to mimic protein filaments on the cellular and molecular level. Maier and his co-workers[137] presented the fabrication of self-assembled helical DNA tubes with widely controllable diameters. The authors suggested that their system give the possibility of large-scale production of biocompatible helical structures with precise control of their diameter and chirality.

Sellner *et al.*[132] presented the possibility of using DNA-based systems as targeted carriers for glucocorticoid dexamethasone (Dex) pH-dependent delivery into MH-S macrophages, with reduced off-target effects. Nanotubes were internalized by macrophages (*in vitro*) and *in vivo* by tissue resident macrophages in mouse cremaster muscles and localized inside their endosomes. *In vitro* tests showed that nanotubes significantly reduced LPS-induced TNF secretion by macrophages. Results were compared with the equivalent amount of free dexamethasone which was not affecting cell viability. Additionally, nanotubes injected into postischemic muscle tissue reduced the ischemia-reperfusion-elicited leukocyte transmigration, as well as the vascular expression of the endothelial adhesion molecules ICAM-1 and VCAM-1.

Li *et al.*[138] presented a study on the *in vivo* stability of DNA structures showing that DNA nanorobots are promising structures applied for precise drug delivery in cancer therapy. They used DNA origami for designing an autonomous DNA robot, which can be programmed to transfer payloads released in tumours. DNA nanorobots are functionalized by DNA aptamers with binded nucleolin outside of their structure, and by the blood coagulation protease thrombin inside it. The *in vivo* tests with tumour-bearing mice showed that DNA nanorobots intravenously injected delivered thrombin specifically into tumour associated blood vessels, furthermore intravascular thrombosis was induced, causing necrosis in the tumour and inhibiting the growth of it.

Methods of analysis

In this section, we review the most common techniques used to evaluate the motion of nanoobjects in fluids, such as Dynamic Light Scattering (DLS), Nanoparticle Tracking Analysis (NTA), and a very promising technique – Optical Tweezers (OT). Most importantly, we emphasize a very important, and unfortunately often ignored fact: these techniques have not been designed for evaluating the size of non-spherical particles (fibres), but for determining their mobility.

Dynamic light scattering

Dynamic light scattering is one of the most popular methods used to determine the particle hydrodynamic size. This method is based on the measurement of changes in the speckle pattern produced by the scattered light of particles during their Brownian motion. An intensity autocorrelation function $G_2(\tau)$ is produced by monodisperse suspensions, and can be described by the equation[139] (eqn (12) and (13)):

$$G_2(\tau) = A\left[1 + B\mathrm{e}^{\left(-2D_q{}^2\tau\right)}\right] \quad (12)$$

$$q = (4\pi n/\lambda)\sin(\theta/2) \quad (13)$$

where: τ – the time delay between intensity measurements; A and B – the baseline and intercept of the correlation function; D – the diffusion coefficient; n – the refractive index of the solvent; λ – the laser wavelength; and θ – the scattering angle.

In the case of a monodisperse system, the diffusion coefficient is related to the hydrodynamic diameter d_h, and is calculated by the Stokes–Einstein equation[139] (eqn (14)):

$$d_\mathrm{h} = \frac{k_\mathrm{B}T}{3D\pi\eta} \quad (14)$$

where: k_B – the Boltzmann constant, T – absolute temperature, and η – the viscosity of the medium.

In the case of a polydisperse sample, the sum of the exponential decays of the different populations of particles (which are present in the sample) describes the correlation function. Due to the ill-posed nature of the Laplace inversion of this correlation function, the obtained decay rate distribution suffers from low resolution.[139,140]

When the light hits the moving Brownian particle, it changes its wavelength due to the Doppler shift. This change

is connected with the particle size. It is possible to calculate the size distribution for spheroidal particles by evaluating the particle diffusion coefficient from the autocorrelation function.[141] The size of the particles is determined by the fluctuations of scattered light intensity caused by the particles' Brownian movements. This technique is very sensitive to the presence of large particles, because the scattered light intensity is proportional to the sixth power of the particle diameter.[139] When the goal is to detect small amounts of large particles this can be an advantage, but if we want to accurately determine size, it can be a major disadvantage. Small amounts of large aggregates or even dust particles can make the size determination difficult, especially when the main component of the analysed colloid is characterized by a significantly smaller size (Fig. 9(c)).[142] However, its high throughput and its easy use have made DLS one of the simplest and most common techniques for the determination of particle size distributions.[139]

With DLS' help, we are able to determine the value of the diffusion coefficients of the studied objects with elongated shape. Wu *et al.* was one of the first to use DLS for the determination of the diffusion coefficient for polymer nanofibres.[143] In their study they used a combination of dynamic and static laser light scattering for determining the mass and composition of such novel polymer nanofibres (the self-assembled cylindrical phase of polystyrene and polystyrene-*b*-poly(2-cinnamoylethyl methacrylate)) and their conformation in solutions. They also tried to determine the diameter and length of these objects using DLS. Wagner and colleagues conducted similar studies.[144] They presented a strategy of a dual-component design for the engineering of self-assembling peptides by using hydrophobic interactions. This strategy had the purpose of facilitating electrostatic forces and axial assembly to regulate the lateral assembly in the process of nanorope formation. Circular dichroism spectropolarimetry experiments showed that their system fulfils the tenet of nanoengineering: the reversible regulation of self-assembly using a variety of mechanisms (*e.g.* temperature or

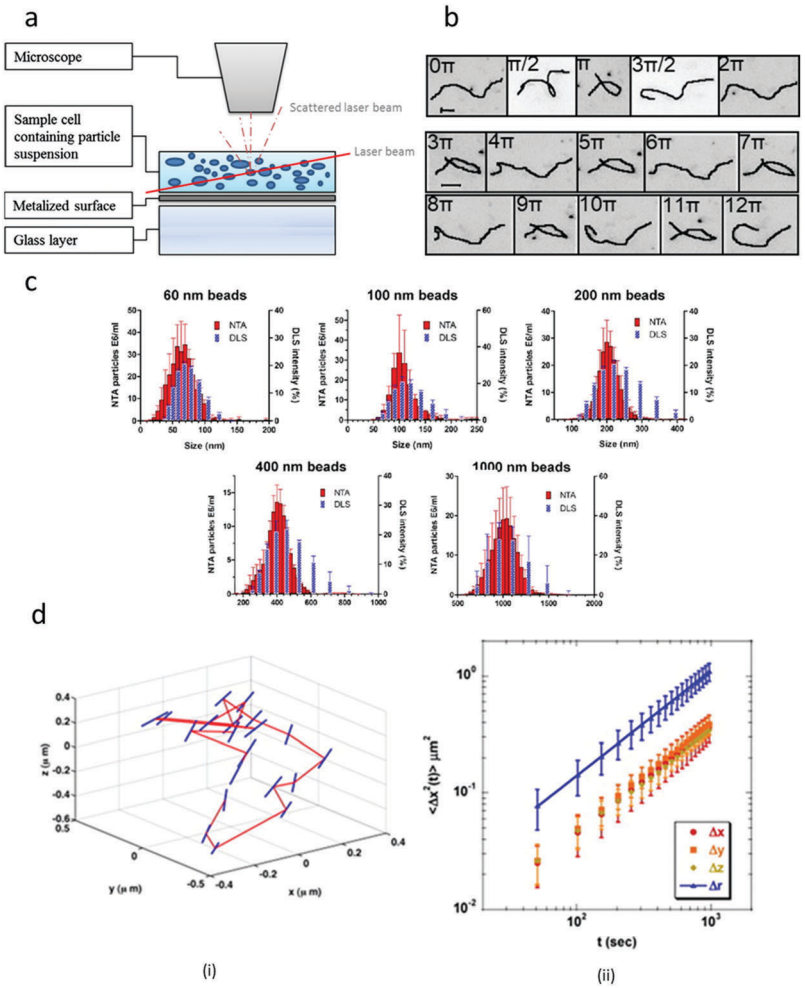

Fig. 9 Analysis of nanoobject tracking: (a) schematic illustration of the NTA system; (b) image analysis of the behaviour and shape conformation change of flexible hydrogel nanofilaments under an oscillating flow; (c) comparison of results of particle hydrodynamic size estimated analysing the object's Brownian motion by DLS and NTA; and (d) 3D projection (i) and mean square displacement (ii) of the elongated vector translational and rotational Brownian motion. Image (a) is reprinted from Gross *et al.*[149] with permission. Image (b) is reprinted from Pawłowska *et al.*[75] with permission. Image (c) is reprinted from Filipe *et al.*[142] with permission. Image (d) is reprinted from Mukhija *et al.*[154] with permission.

solvent factors). In their experiments they used DLS for the confirmation of self-assembled polymers in a solution and to calculate the diffusion of elongated polymer nanomaterials. Their direct purpose was to determine, on this basis, average diameters and lengths of polymer nanofilaments. While in the case of spherical particles the use of a commercial DLS technique to determine hydrodynamic diameters is the most reasonable, this approach is of course wrong when we are dealing with objects with an elongated shape like filaments. Determining the physical diameter and length for these objects becomes impossible. Sugihara and Kavitha with co-workers similarly misinterpreted the data obtained.

Sugihara *et al.*[145] analysed cross-linked biomimetic diblock copolymers PMPC–PHPMA prepared by RAFT aqueous dispersion polymerization. For polymer characterization they used gel permeation chromatography, ^{1}H NMR spectra, DLS and AFM measurements, and TEM analysis. They showed that the use of higher levels of EGDMA led to increasing anisotropy of this particle, with both a worm-like morphology and a novel ''lumpy rod'' morphology. Kavitha *et al.*[146] synthesized and characterized polyaniline nanofibres. They used XRD, SEM, TEM, and DLS techniques to determine the size and morphology of these polymers. Small-angle neutron scattering (SANS) was used to find different parameters of crystalline polymer nanofibre particles. Unfortunately, the DLS data obtained were misinterpreted by the authors. They claimed that the two peaks in the size distribution of the examined objects correspond to diameter and length, which is obviously an erroneous assumption, because DLS analysis simply describes an elongated particle as a spherical object with an equivalent hydrodynamic behaviour and does not allow one to distinguish between the longer and the shorter axis of the object.

Very interesting results were obtained by Levin *et al.* who, in their research on non-spherical nanoobjects, used the new DLS-based technique called ''multipolarization dynamic light scattering'' (MS DLS).[147] This technique is based on time-resolved measurements of the scattered light intensity at different angles between the incident and scattered light polarizations. The estimated translational and rotational diffusion coefficients of the analysed object, in relation to the intensity of the autocorrelation function, make it possible to determine its diameter and length. The authors presented a detailed description of the method and described its physical foundations. They also described the new data processing and implementation algorithm, together with the experimental results of non-spherical nanoparticle sizing and etching-induced size changing. This MS DLS technique seems very promising and can be very helpful in determining the hydrodynamic size of cylindrical particles like elongated polymeric nanoobjects.

Single nanoobject tracking analysis

Nanoparticle tracking analysis is a technique used for the simultaneous detection of sub-micron particle size distributions and concentrations of particles in a sample (Fig. 9(a and c)).[141] The particle size ranges from a few nanometres to more than 2 μm in diameter.[142,148] NTA has been used for various applications in different research and industry fields, and also for various sample compositions, such as virus particles, gold nanoparticle conjugation, cellular vesicles, fullerenes or proteins, microvesicles, and exosomes.[141,149,150] This technique permits the multi-parameter and simultaneous real-time analysis of the size distribution of nanoparticles in liquid suspensions and their concentration.[149]

In a typical experiment, the liquid sample is pumped into a sample chamber that is illuminated by a laser. A camera records the particle movement by tracking the light-scattering centres of the particles. Thanks to this, the Brownian motion of the particles is analysed in real time. Each particle is simultaneously but individually visualised and tracked by a specific software program for image tracking. The diffusion coefficient of all the tracked particles is calculated based on the Stokes–Einstein equation. It is possible to calculate the particle size (hydrodynamic diameter) for each spheroidal particle.[149] Particle size and concentration can be measured using light scattering, while a fluorescence mode provides the differentiation of naturally fluorescing or labelled particles.[148] The software of the nanoparticle tracking analysis permits identifying and tracking individual nanomaterials moving under the influence of Brownian motion, while the results make it possible to recover the particle number concentration.[150]

NTA presents many advantages in relation to particle detection, compared to other methods such as dynamic light scattering.[142,149,151] The main advantage of NTA is the direct and real-time visualisation of particle movements. It provides simultaneous counting, sizing, and Brownian motion of nanoparticles. When we compare it with DLS, we can see that NTA provides a slightly better quantification and resolution of the different size populations of the detected particles. In addition, Haw van der Pol *et al.* have shown that differences in the refractive index can be helpful to differentiate single nanoparticle populations by size, as well as by their scattering intensity.[152] Another advantage of NTA is its flexibility but, at the same time, that is connected with a variability in parameter settings: a feature that could be considered a disadvantage of this technique.[142,149] The techniques based on light scattering principles show significant complexity in the context of correct result interpretation. NTA is a valuable technique to gain better insight into the quantitative analysis of particle suspensions.[149]

The measurement of the particles suspended in liquid is still a big challenge, especially in the case of polymodal, highly polydisperse samples. The NTA technique presents new opportunities and has high potential compared to other methods. Thanks to this technique it is possible to obtain reproducible good results in detecting particle concentrations, size distributions, and dynamics for mono- and bimodal particle suspensions, as long as we know the sample composition.[149]

Despite the difficulties connected with non-spherical objects (and related anisotropic behaviour), the NTA technique has been used to analyse elongated nanomaterials. Mehtala and Wei used NTA to characterize the hydrodynamic size and stability of ligand-coated nanorods.[153] The authors stated that the precision of NTA is sufficient to permit differences in the

hydrodynamic size of nanorods to be interpreted in terms of surfactant conformation and structure. The hydrodynamic diameter values obtained from NTA correlate closely with the gold nanorod length, with greater accuracy and precision than with DLS, and with a comparable resolution to TEM. Mukhija *et al.* also used a particle tracking confocal microscopy method to characterize the translational and orientational dynamics of colloidal rods with three-dimensional resolution (Fig. 9(d)).[154] Their method relies on solvent viscosification to retard dynamics to time scales that are compatible with 3D confocal optical microscopy. The authors applied this method to suspensions of colloidal rods undergoing Brownian motion and found that the measured rotational and translational diffusion coefficients agree well with the theory applying to infinite dilution. Rod translational and rotational diffusivities are extracted from the measured translational mean square displacement of centroid positions and the rod unit vector $\mathbf{u}(t)$, respectively. Additionally, the results obtained permit suggesting that the ability of the method to simultaneously resolve three spatial and two orientational dimensions offers potential applications for studying the dynamics of complex particles that combine anisotropy in shape and potential interactions. Tracking analysis proved to be an equally useful technique for analysing the mobility of biopolymer nanofilaments.

Ruhnow and his co-workers combined their algorithm capable of localizing, with nanometric precision, the centrelines and tips of curved filaments with single-particle tracking methods to create so-called Fluorescence Image Evaluation Software for Tracking and Analysis.[155] They presented this algorithm to precisely localize curved filaments – whose structures are characterized by subresolution diameters and micrometre lengths – by using surface-immobilized microtubules.

All the works described above investigated materials that were quite rigid, but the situation is even more complex when elongated nanomaterials are flexible. In our study we presented an investigation into the mobility of highly flexible hydrogel nanofilaments in Brownian conditions[18] (Fig. 4(c)) and in an environment which simulates the intercellular and inter-tissue flow in living organisms (Fig. 9(b)).[75] Our experimental data showed that flexible nanofilaments are proper tools for investigating Brownian motion, folding dynamics, and bending of elongated deformable objects. We could conclude that the diffusion coefficients obtained for such objects generally differ from the theoretical predictions based on a drag force for stiff ellipsoidal nanorods. The observation of flexible nanofilaments during the long time span under the influence of Brownian dynamics, as well as under an oscillatory flow, provided the opportunity to estimate their elasticity (Young's modulus, relative extensional stiffness, and relative flexural stiffness). This technique enables us to study all types of diffusion, coiling and uncoiling processes, orientation, and cross-flow migration.[75]

Optical tweezers

Optical tweezers are a technique capable of trapping small particles using the forces generated by laser radiation pressure. It can be used to manipulate and study the motion of single colloidal particles, cells, and molecules measuring in the range from a few nanometres to a few micrometers, and to analyse the physical and rheological properties of these materials.[156–159] Up until the 1960s it was not possible to use the radiation pressure generated by light to modify the position of matter, but in those years the advent of lasers provided a light source with the appropriate properties for generating a light trap. The subsequent rise of nanotechnology provided the opportunity to synthesize, modify, and control materials on the nanometric scale. These two factors opened the way for optical trapping. Arthur Ashkin is the developer of the "single-beam gradient force trap", the technique that we call optical tweezers.[160] In the 1970s Ashkin studied the interactions between micromaterials and light, and was able to trap particles in a confined three-dimensional space using the forces of light radiation. In the following years, Ashkin was able to demonstrate that forces on the piconewton scale can be applied on small dielectric microspheres by highly focused laser beams using a high numerical aperture microscope objective.[161]

One of the fundamental requirements of this system is the use of particles having a higher index of refraction than their neighbouring medium. The index of refraction ratios should be higher than 1.1. According to Snell's law, when the light coming from a medium passes into a dielectric material with a low refractive index, its rays are deflected. Optical tweezers stand out for their high resolution, sensitivity, and flexibility.[162] By using this instrument it is possible to detect subnanometric displacements and to measure femtonewton forces. Furthermore, their non-invasive character plays an important role in new types of biomaterials.

Initially, the scope of OT applications included physical and biological science. Currently, this technique is used as an emerging method to investigate rheological phenomena. As was mentioned by Yao *et al.*, optical tweezers are a good technique for studying the active microrheology of nano- and microobjects.[163] The majority of microrheological techniques are based on the observation of the free or driven motion of tracer particles introduced into the fluid under investigation.

Beyond spherical particles, optical tweezers are capable of trapping particles with wildly varying geometries and compositions, *e.g.* elongated polymers. Simpson[164] has qualitatively discussed the origins and variety of optical forces that can be applied to anisotropic and inhomogeneous particles by tightly focused beams of light (Fig. 10(a)).

The author emphasizes that optical tweezers became a powerful tool for conducting fundamental rheological research. Marago and his co-workers showed that it is possible to control the trapping of even more complex nanostructures (Fig. 10(b)).[165] The authors reviewed the state-of-the-art in optical trapping at the nanoscale, with an emphasis on some of the most promising advances, such as controlled manipulation and assembly of individual and multiple nanostructures, force measurement with femtonewton resolution, and biosensors. In their opinion, the optical manipulation of individual nanoparticles will play a crucial role in the development and characterization of single nano- and microobjects in fluids. In recent years several studies have focused on the dynamics of elongated nanoparticles. For example,

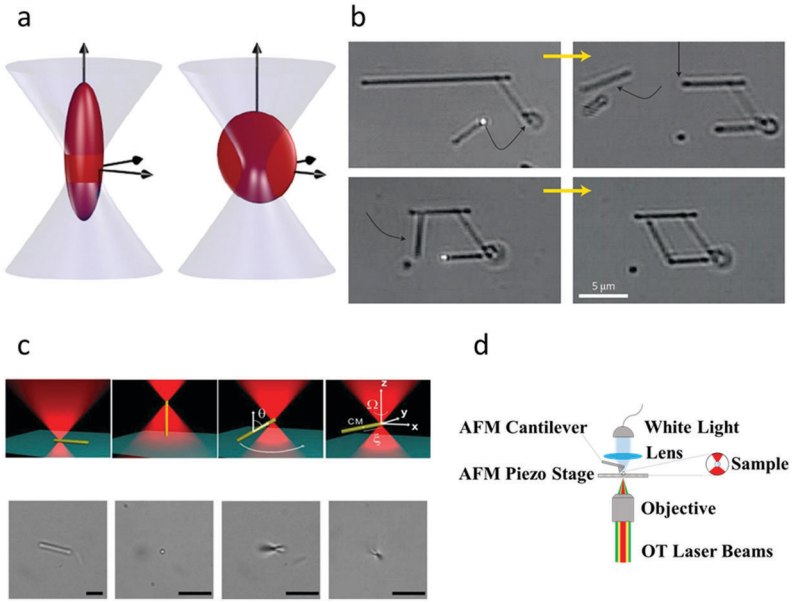

Fig. 10 Applications of optical tweezers: (a) trapping of spherical (right) and elongated (left) particles, the arrows represent the trapped object symmetry axis and the laser beam axis; (b) scheme of the manipulation of nanowires using optical force in order to obtain a desired structure; (c) trapping and rotation of polymer fibres (scale bar 2.5 μm); and (d) scheme of the AFM/OT. Image (a) is reprinted from Simpson *et al.*[164] with permission. Image (b) is reprinted from Marago *et al.*[165] with permission. Image (c) is reprinted from Neves *et al.*[167] with permission. Image (d) is reprinted from Pierini *et al.*[171] with permission.

Hajizadeh *et al.* analysed the Brownian motion of a rotating nanorod by optical tweezers.[166] They showed that, for typical settings, the effective rotational and translational fluctuations are drastically different. Interestingly, researchers suggested that translational dynamics can have a non-negligible influence on rotational fluctuations due to the small size of a nanorod in comparison to the focal spot. Neves *et al.* showed experimental Q15 evidence of rotation of tilted polymer nanofibres fabricated by the electrospinning technique, using a highly focused linear polarized Q16 Gaussian beam.[167] The authors demonstrated the optical trapping and manipulation of polymer electrospun nanofibres, introducing control over the rotation of these elongated nanostructures by tilting the trapped fibres (Fig. 10(c)). They compared experimental rotation frequencies to calculations based on the T-matrix formalism, which accurately reproduces measured data, thus providing a comprehensive description of the rotation dynamics of linear nanostructures.

OT are useful for looking at nanomaterial behaviour from a new perspective by analysing the ballistic motion of Brownian particles in a liquid. Huang *et al.* reported observation of the Brownian motion of a single particle in an optical trap and sub-Ångström spatial precision, and the determination of the particle's velocity autocorrelation function.[168] Their observation was the first measurement of the ballistic Brownian motion of a particle in a liquid. The data are in excellent agreement with the theoretical predictions which take into account the inertia of the particle and hydrodynamic memory effects.

What is very important and extremely promising is the fact that optical tweezers can be combined with microfluidic chips to study nanomaterial behaviour not only in the Brownian condition but under the influence of an external flow as well, as has been confirmed by Boer *et al.*[169] In their work, an array of four independent laser traps was combined with a polydimethylsiloxane microfluidic chip to form a very compact system permitting the parallel processing of biological objects. By pressure control of the inlet flows, the trapped objects can be put in contact with different solutions for analysis purposes. Their setup, including a fluorescence excitation–detection scheme, offers the potential to perform complex biochemical manipulations on an ensemble of microparticles. OT studies in flow can be quite complicated for elongated nanomaterials. Ahmed and Sung attempted to investigate the stabilities of spherical and non-spherical particles with diameters smaller than the wavelength of the trapping light when the system encounters a fluid flow.[170] Optical trapping forces on elongated particles were examined for various flow conditions. It was found that the stability of non-spherical particles is significantly affected by the fluid velocity and the orientation of particles. Other authors showed that the length of the particle in the transverse direction also had a significant impact on particle stability.

A completely new and highly beneficial approach in new technological applications led to the development of hybrid OT instruments (Fig. 10(d)) which make it possible to perform typical OT experiments as well as high-resolution imaging and mechanical indentation testing.[171] This instrument combining atomic force microscopy with optical tweezers (AFM/OT) has Q17 high potential in nanomechanics, molecule manipulation, and biological studies. It is a high-quality imaging instrument capable of trapping and modifying nanometric materials as well as of measuring forces on the subpiconewton scale.

The experiments conducted proved that this instrument can be useful either as a nanomanipulator or for studying nano- and micromaterial movements and related forces and, at the same time, be able to scan the examined structure with the AFM probe, thus generating high resolution images of the manipulated sample.

Conclusions and outlook

The current dynamic development of nanotechnologies contributes to numerous new products in various sectors of science and industry. Nano-scale objects have become prevalent among theoreticians and experimentalists from several disciplines (chemistry, biology, engineering, and medicine). Their small size creates new opportunities for the application of spherical and elongated nanoobjects as targeted drug carriers and biomaterials for tissue engineering. Such systems make it possible to deliver drugs to specific organs, tissues, and cells within the body to obtain the targeted action. An important issue is the construction of proper nanocarriers, allowing for their controllable transport within tissue and cell environments.

In this review, we presented the most significant biomedical applications of polymeric nanofibers highlighting the importance of knowing the behaviour of such materials inside the living organism, therefore, a detailed overview of the dynamics of elongated nanoobjects suspended in fluid was presented.

There are several techniques useful for fabricating polymer fibres for biomedical applications, among them electrospinning (including coaxial electrospinning) and the solution blow spinning process stand out from the crowd due to their unique potential to obtain fibres with nanoscale diameters. We also highlighted a few interesting fibre cutting methods that allow obtaining short nanofilaments from fibrous mats. As an alternative to fibres made of artificial polymers, DNA nanostructures have gained interest among researchers investigating new objects as drug release systems, and such structures have shown promising properties in both *in vitro* and *in vivo* tests.

A typical body fluid flow is non-Newtonian in nature, which strongly affects the conformation and properties of elongated and deformable nanoobjects. Under the flow, these objects are oriented, deformed, and coiled, thus leading to a macroscopic variation of the transport properties. The microscopic structure, as well as the macroscopic response, depend on both the nature of the suspended objects and the geometry of the viscous flow. Linking mechanical and microscopic properties of the suspended objects to the macroscopic response of the suspension is one of the fundamental scientific challenges of soft matter physics which remains unsolved for a large number of situations.

The most interesting methods of analysis of polymer nanoobject behaviour in flow have also been presented. DLS and NTA are widely used to determine the spherical colloidal system size distribution, while it should be pointed out that these methods allow one to determine elongated object mobility in Brownian conditions too. Optical tweezers-based methods have been recently highly appreciated in this field, because they allow one to precisely study the forces acting between a single nanoobject and its surrounding environment. In addition, we focused on the combination of optical tweezers with atomic force microscopy which opens new possibilities for trapping and modifying nanometric materials as well as of measuring forces at the subpiconewton scale.

In conclusion, understanding the relationship between particle or filament structure and behaviour and macroscopic flow properties opens the door to designing nanoobjects which could be effectively transported by body fluids for dedicated drug release and/or local tissue regeneration. Q18

Conflicts of interest

There are no conflicts of interest to declare.

Acknowledgements

This work was financially supported by the National Centre for Research and Development (NCBiR grant no. LIDER/28/0067/L-7/15/NCBR/2016) and the Polish National Science Centre (NCN, grant no. 2015/17/N/ST8/02012).

References

1 I. Yu, T. Mori, T. Ando, R. Harada, J. Jung, Y. Sugita and M. Feig, *eLife*, 2016, **5**, e19274.
2 M. Feig, I. Yu, P. Wang, G. Nawrocki and Y. Sugita, *J. Phys. Chem. B*, 2017, **121**, 8009.
3 S. Cheng, M. Cetinkaya and F. Gräter, *Biophys. J.*, 2010, **99**, 3863.
4 Encyclopaedia Britannica, Inc., www.britannica.com/science/white-blood-cell, accessed May 2018.
5 J. Shin, A. G. Cherstvy and R. Metzler, *Soft Matter*, 2015, **11**, 472.
6 O. C. Farokhzad and R. Langer, *ACS Nano*, 2009, **3**, 16.
7 K. Bogunia-Kubik and M. Suguisaka, *BioSystems*, 2002, **65**, 123.
8 Z. Wang, *Theranostics*, 2016, **6**, 2431.
9 A. Samborski, P. Jankowski, J. Węgrzyn, J. A. Michalski, S. Pawłowska, S. Jakieła and P. Garstecki, *Eng. Life Sci.*, 2015, **15**, 333.
10 F. Sonvico, C. Dubernet, P. Colombo and P. Couvreur, *Curr. Pharm. Des.*, 2005, **11**, 2091.
11 T. Okudaa, K. Tominagab and S. Kidoaki, *J. Controlled Release*, 2010, **143**, 258.
12 P. Dayal, J. Liu, S. Kumar and T. Kyu, *Macromolecules*, 2007, **40**, 7689.
13 J. Wanigasekara and C. Witharana, *Curr. Trends Biotechnol. Pharm.*, 2016, **10**, 78.
14 R. Colognato, M. V. D. Z. Park, P. Wick and W. H. De Jong, *Adverse Effects of Engineered Nanomaterials*, Elsevier Inc., 2012.
15 J. Xie and C. H. Wang, *Pharm. Res.*, 2006, **23**, 1817.

16 Y. Z. Zhang, C. T. Lim, S. Ramakrishna and Z.-M. Huang, *J. Mater. Sci.: Mater. Med.*, 2005, **16**, 933.
17 G. Verreck, I. Chun, J. Rosenblatt, J. Peeters, A. V. Dijck, J. Mensch, M. Noppe and E. Brewster, *J. Controlled Release*, 2003, **92**, 349.
18 P. Nakielski, S. Pawlowska, F. Pierini, V. Liwinska, P. Hejduk, K. Zembrzycki, E. Zabost and T. A. Kowalewski, *PLoS One*, 2015, **10**, e0129816.
19 W. Cui, Y. Zhou and J. Chang, *Sci. Technol. Adv. Mater.*, 2010, **11**, 014108.
20 L. S. Nair, S. Bhattacharyya and C. T. Laurencin, *Expert Opin. Biol. Ther.*, 2004, **4**, 659.
21 Z. M. Huang, C. L. He, A. Yang, Y. Zhang, X. J. Han, J. Yin and Q. Wu, *J. Biomed. Mater. Res., Part A*, 2006, **77**, 169.
22 N. Bölgen, I. Vargel, P. Korkusuz, Y. Z. Menceloğlu and E. Pişkin, *J. Biomed. Mater. Res., Part B*, 2007, **81**, 530.
23 H. Nie and C. H. Wang, *J. Controlled Release*, 2007, **120**, 111.
24 H. Jiang, Y. Hu, P. Zhao, Y. Li and K. Zhu, *J. Biomed. Mater. Res., Part B*, 2006, **79**, 50.
25 D. Liang, Y. K. Luu, K. Kim, B. S. Hsiao, M. Hadjiargyrou and B. Chu, *Nucleic Acids Res.*, 2005, **33**, e170.
26 T. J. Sill and H. A. von Recum, *Biomaterials*, 2008, **29**, 1989.
27 A. L. Yarin, B. Pourdeyhimi and S. Ramakrishna, *Fundamentals and Applications of Micro- and Nanofibers*, Cambridge University Press, Cambridge, 2014.
28 R. Srikar, A. L. Yarin, C. M. Megaridis, A. V. Bazilevsky and E. Kelley, *Langmuir*, 2008, **24**, 965.
29 M. Gandhi, R. Srikar, A. L. Yarin, C. M. Megaridis and R. A. Gemeinhart, *Mol. Pharmaceutics*, 2009, **6**, 641.
30 S. Khansari, S. Duzyer, S. Sinha-Ray, A. Hockenberger, A. L. Yarin and B. Pourdeyhimi, *Mol. Pharmaceutics*, 2013, **10**, 4509.
31 D. Howard, L. D. Buttery, K. M. Shakesheff and S. J. Roberts, *J. Anat.*, 2008, **213**, 66.
32 A. Tamayol, M. Akbari, N. Annabi, A. Paul, A. Khademhosseini and D. Juncker, *Biotechnol. Adv.*, 2013, **31**, 669.
33 C. D. Markert, X. Guo, A. Skardal, Z. Wang, S. Bharadwaj, Y. Zhang, K. Bonin and M. Guthold, *J. Mech. Behav. Biomed. Mater.*, 2013, **27**, 115.
34 S. Mukherjee, C. Gualandi, M. L. Focarete, R. Ravichandran, J. R. Venugopal, M. Raghunath and S. Ramakrishna, *J. Mater. Sci.: Mater. Med.*, 2011, **22**, 1689.
35 M. M. Stevens and J. H. George, *Science*, 2005, **310**, 1135.
36 M. Pokrywczyńska, A. Jundziłł, J. Adamowicz, T. Kowalczyk, K. Warda, M. Rasmus, Ł. Buchholz, S. Krzyżanowska, P. Nakielski, T. Chmielewski, M. Bodnar, A. Marszałek, R. Dębski, M. M. Frontczak-Baniewicz, G. Mikułowski, M. Nowacki, T. A. Kowalewski and T. Drewa, *PLoS One*, 2014, **9**, e105295.
37 T. Kloskowski, A. Jundziłł, T. Kowalczyk, M. Nowacki, M. Bodnar, A. Marszałek, M. Pokrywczyńska, M. M. Frontczak-Baniewicz, T. A. Kowalewski, P. Chłosta and T. Drewa, *PLoS One*, 2014, **9**, e106023.
38 A. Subramanian, U. M. Krishnan and S. Sethuraman, *J. Biomed. Sci.*, 2009, **16**, 108.
39 P. Nakielski, T. Kowalczyk, K. Zembrzycki and T. A. Kowalewski, *J. Biomed. Mater. Res., Part B*, 2015, **103**, 282.
40 C. E. Schmidt and J. B. Leach, *Annu. Rev. Biomed. Eng.*, 2003, **5**, 293.
41 F. Yang, R. Murugan, S. Wang and S. Ramakrishna, *Biomateriale*, 2005, **26**, 2603.
42 L. E. Freed, G. Vunjak-Novakovic, R. J. Biron, D. B. Eagles, D. C. Lesnoy, S. K. Barlow and R. Langer, *Nat. Biotechnol.*, 1994, **12**, 689.
43 S. Stratton, N. B. Shelke, K. Hoshino, S. Rudraiah and S. G. Kumbar, *Bioact. Mater.*, 2016, **1**, 93.
44 S. Grad, L. Kupsik, K. Gorna, S. Gogolewski and M. Alini, *Biomaterials*, 2003, **24**, 5163.
45 D. A. Grande, C. Halberstadt, R. Schwarz and R. Manji, *J. Biomed. Mater. Res.*, 1997, **34**, 211.
46 G. Chen, T. Sato, H. Ohgushi, T. Ushida, T. Tateishi and J. Tanaka, *Biomaterials*, 2005, **26**, 2559.
47 J. K. Wise, A. L. Yarin, C. M. Megaridis and M. Cho, *Tissue Eng.*, 2009, **15**, 913.
48 B. Rentsch, A. Hofmann, A. Breier, C. Rentsch and D. Scharnweber, *Ann. Biomed. Eng.*, 2009, **37**, 2118.
49 A. Ortega and J. Garcia de la Torre, *J. Chem. Phys.*, 2003, **119**, 9914.
50 J. Philibert, *Diffus. Fundam.*, 2006, **4**, 6.1.
51 S. R. de Groot and P. Mazur, *Nonequilibrium thermodynamics*, North Holland Publishing Company, Amsterdam, 1962.
52 M. A. Charsooghi, E. A. Akhlaghi, S. Tavaddod and H. R. Khalesifard, *Comput. Phys. Commun.*, 2011, **182**, 400.
53 A. J. Levine, T. B. Liverpool and F. C. MacKintosh, *Phys. Rev. E: Stat., Nonlinear, Soft Matter Phys.*, 2004, **69**, 021503.
54 A. Loman, I. Gregor, C. Stutz, M. Mundb and J. Enderlein, *Photochem. Photobiol. Sci.*, 2010, **9**, 627.
55 O. Kratky and G. Porod, *Recl. Trav. Chim. Pays-Bas*, 1949, **68**, 1106.
56 H. Yamakawa, *Modern theory of polymer solutions*, Harper & Row Publishers, New York, 1971.
57 P. LeDuc, C. Haber, G. Bao and D. Wirtz, *Nature*, 1999, **399**, 564.
58 M. Bukowicki and M. L. Ekiel-Jeżewska, *Soft Matter*, 2018, **14**, 5786.
59 R. Herczynski, *Arch. Mech.*, 2016, **68**, 81.
60 D. Tsvirkun, A. Grichine, A. Duperray, C. Misbah and L. Bureau, *Sci. Rep.*, 2017, **7**, 45036.
61 G. Segre and A. Silberberg, *Nature*, 1961, **189**, 209.
62 F. J. Gauthier, H. L. Goldsmith and S. G. Mason, *Biorheology*, 1972, **9**, 205.
63 P. C. H. Chan and L. G. Leal, *J. Fluid Mech.*, 1979, **92**, 131.
64 W. Hiller and T. A. Kowalewski, *Exp. Fluids*, 1987, **5**, 43.
65 H. A. Stone, *Annu. Rev. Fluid Mech.*, 1994, **26**, 65.
66 S. Mortazavi and G. Tryggvason, *J. Fluid Mech.*, 2000, **411**, 325.
67 X. Chen, Ch. Xue, L. Zhang, G. Hu., X. Jiang and J. Sun, *Phys. Fluids*, 2014, **26**, 112003.
68 C. A. Stan, L. Guglielmini, A. K. Ellerbee, D. Caviezel, H. A. Stone and G. M. Whitesides, *Phys. Rev. E: Stat., Nonlinear, Soft Matter Phys.*, 2011, **84**, 036302.

69 K. Chaudhury, S. Mandal and S. Chakraborty, *Phys. Rev. E*, 2016, **93**, 023106.
70 T. V. Starkey, *Br. J. Appl. Phys.*, 1956, **7**, 52.
71 A. Brandt and G. Bugliarello, *Trans. Soc. Rheol.*, 1966, **10**, 229.
72 A. D. Maude and J. A. Yearn, *J. Fluid Mech.*, 1967, **30**, 601.
73 A. M. Słowicka, M. L. Ekiel-Jeżewska, K. Sadlej and E. Wajnryb, *J. Chem. Phys.*, 2012, **136**, 044904.
74 A. M. Słowicka, E. Wajnryb and M. L. Ekiel-Jeżewska, *Eur. Phys. J. E: Soft Matter Biol. Phys.*, 2013, **36**, 1.
75 S. Pawłowska, P. Nakielski, F. Pierini, I. K. Piechocka, K. Zembrzycki and T. A. Kowalewski, *PLoS One*, 2017, **12**, e0187815–1.
76 K. Sadlej, E. Wajnryb, M. L. Ekiel-Jezewska, D. Lamparska and T. A. Kowalewski, *Int. J. Heat Fluid Flow*, 2010, **31**, 996.
77 B. P. Ho and L. G. Leal, *J. Fluid Mech.*, 1974, **65**, 365.
78 G. B. Jeffery, *Proc. R. Soc. London, Ser. A*, 1922, **102**, 161.
79 L. C. Nitsche and E. J. Hinch, *J. Fluid Mech.*, 1997, **332**, 1.
80 H. Amini, W. Lee and D. Di Carlo, *Lab Chip*, 2014, **14**, 2739.
81 D. R. Steinhauser, PhD thesis, Georg August University, 2008.
82 S. Yang and G. Dou, *Phys. Fluids*, 2005, **17**, 065104.
83 G. H. Michler and F. J. Balta-Calleja, *Mechanical properties of polymers based on nanostructure and morphology*, Taylor & Francis Group, 2005.
84 S. R. Baker, S. Banerjee, K. Bonin and M. Guthold, *Mater. Sci. Eng., C*, 2016, **59**, 203.
85 N. Mücke, K. Klenin, R. Kirmse, M. Bussiek, H. Herrmann, M. Hafner and J. Langowski, *PLoS One*, 2009, **4**, e7756.
86 S. E. Bresler and Y. I. Frenkel, *Zh. Eksp. Teor. Fiz.*, 1939, **9**, 1094.
87 M. J. Quevillon, Bachelor thesis, University of Minnesota-Twin Cities, 2015.
88 J. S. Graham, B. R. McCullough, H. Kang, W. A. Elam, W. Cao and E. M. De La Cruz, *PLoS One*, 2014, **9**, e94766.
89 T. B. Liverpool, *Philos. Trans. R. Soc., A*, 2006, **364**, 3335.
90 G. Lamour, J. B. Kirkegaard, H. Li, T. P. J. Knowles and J. Gsponer, *Source Code Biol. Med.*, 2014, **9**, 1–6.
91 F. Gittes, B. Mickey, J. Nettleton and J. Howard, *J. Cell Biol.*, 1993, **120**, 923.
92 E. J. Janson and M. Dogterom, *Biophys. J.*, 2004, **87**, 2723.
93 A. Ott, M. Magnasco, A. Simon and A. Libchaber, *Phys. Rev. E: Stat. Phys., Plasmas, Fluids, Relat. Interdiscip. Top.*, 1993, **48**, R1642.
94 M. Doi and S. F. Edwards, *The theory of polymer dynamics*, Oxford Science Publications, New York, 1986.
95 S. Pawłowska, PhD thesis, Institute of Fundamental Technological Research Polish Academy of Sciences, 2018.
96 E. S. Medeiros, G. M. Glenn, A. P. Klamczynski, W. J. Orts and L. H. C. Mattoso, *J. Appl. Polym. Sci.*, 2009, **113**, 2322.
97 T. Grafe and K. Graham, *International Nonwovens Technical Conference*, Atlanta, 2002.
98 A. Formalas, *US Pat.*, 1975504, 1934.
99 J. Doshi and D. H. Reneker, *J. Electrost.*, 1995, **35**, 151.
100 D. Li and Y. Xia, *Adv. Mater.*, 2004, **16**, 1151.
101 A. Greiner and J. H. Wendorff, *Angew. Chem., Int. Ed.*, 2007, **46**, 5670.
102 T. A. Kowalewski, S. Błoński and S. Barral, *Bull. Pol. Acad. Sci.: Tech. Sci.*, 2005, **53**, 385.
103 F. Pierini, M. Lanzi, P. Nakielski, S. Pawłowska, O. Urbanek, K. Zembrzycki and T. A. Kowalewski, *Macromolecules*, 2017, **50**, 4972.
104 J. Stanger, N. Tucker, A. Wallace, N. Larsen, M. Staiger and R. Reeves, *J. Appl. Polym. Sci.*, 2009, **112**, 1729.
105 P. Kumar, Bachelor thesis, Rourkela National Institute of Technology, 2012.
106 M. M. Hohman, M. Shin, G. Rutledge and M. P. Brenner, *Phys. Fluids*, 2001, **13**, 2201.
107 F. Pierini, M. Lanzi, P. Nakielski and T. A. Kowalewski, *J. Nanomater.*, 2017, 1.
108 F. Pierini, M. Lanzi, P. Nakielski, S. Pawłowska, K. Zembrzycki and T. A. Kowalewski, *Polym. Adv. Technol.*, 2016, **27**, 1465.
109 A. V. Bazilevsky, A. L. Yarin and C. M. Megaridis, *Langmuir*, 2007, **23**, 2311.
110 Ch. Wang, L. Wang and M. Wang, *Mater. Lett.*, 2014, **124**, 192.
111 H. Qu, S. Wei and Z. Guo, *J. Mater. Chem. A*, 2013, **1**, 11513.
112 D.-G. Yu, J. H. Yu, L. Chen, G. R. Williams and X. Wang, *Carbohydr. Polym.*, 2012, **90**, 1016.
113 M. F. Elahi, W. Lu, G. Guoping and F. Khan, *J. Bioeng. Biomed. Sci.*, 2013, **3**, 1.
114 C. Gualandi, A. Celli, A. Zucchelli and M. L. Focarete, *Adv. Polym. Sci.*, 2015, **267**, 87.
115 J. Díaz, A. Barrero, M. Márquez and I. Loscertales, *Adv. Funct. Mater.*, 2006, **16**, 2110.
116 X. Zhuang, L. Shi, K. Jia, B. Cheng and W. Kang, *J. Membr. Sci.*, 2013, **429**, 66.
117 M. Lee, S. S. Yoon and A. L. Yarin, *ACS Appl. Mater. Interfaces*, 2016, **8**, 4955.
118 B. Eling, S. Gogolewski and A. Pennings, *J. Polym.*, 1982, **23**, 1587.
119 D. D. da Silva Parize, M. M. Foschini, J. E. de Oliveira, A. P. Klamczynski, G. M. Glenn, J. M. Marconcini and L. H. Capparelli Mattoso, *J. Mater. Sci.*, 2016, **51**, 4627.
120 J. E. Oliveira, E. A. Moraes, R. G. F. Costa, A. S. Afonso, L. H. C. Mattoso, W. J. Orts and E. S. Medeiros, *J. Appl. Polym. Sci.*, 2011, **122**, 3396.
121 M. Wojasiński, M. Pilarek and T. Ciach, *Pol. J. Chem. Technol.*, 2014, **16**, 43.
122 A. M. Behrens, B. J. Casey, M. J. Sikorski, K. L. Wu, W. Tutak, A. D. Sandler and P. Kofinas, *ACS Macro Lett.*, 2014, **3**, 249.
123 *Polypropylene: an A-Z reference*, ed. I. E. Spruiell, E. Bond and J. Karger-Kocsis, Kluwer Academic Publishers, Dordrecht, 1999.
124 R. Zhao and L. C. Wadsworth, *Polym. Eng. Sci.*, 2003, **43**, 463.
125 G. Verreck, I. Chun, J. Peeters, J. Rosenblatt and M. E. Brewster, *Pharm. Res.*, 2003, **20**, 810.
126 M. Thieme, S. Agarwal, J. H. Wendorff and A. Greiner, *Polym. Adv. Technol.*, 2011, **22**, 1335.
127 M. Sawawi, T. Y. Wang, D. R. Nisbet and G. P. Simon, *Polymer*, 2013, **54**, 4237.

128 G. Duan, S. Jiang, T. Moss, S. Agarwal and A. Greiner, *Polym. Chem.*, 2016, **7**, 2759.

129 A. G. B. Castro, M. C. Lo Giudice, T. Vermonden, S. C. G. Leeuwenburgh, J. A. Jansen, J. J. J. P. van den Beucken and F. Yang, *ACS Biomater. Sci. Eng.*, 2016, **2**, 2099.

130 S. Jiang, G. Duan, U. Kuhn, M. Mörl, V. Altstädt, A. L. Yarin and A. Greiner, *Angew. Chem., Int. Ed.*, 2017, **56**, 1.

131 I. W. Fathona and A. Yabuki, *J. Mater. Process. Technol.*, 2013, **213**, 1894.

132 S. Sellner, S. Kocabey, T. Zhang, K. Nekolla, S. Hutten, F. Krombach, T. Liedl and M. Rehberg, *Biomaterials*, 2017, **134**, 78.

Q19 133 Q. Hu, H. Li, L. Wang, H. Gu and C. Fan, *Chem. Rev.*, 2018, in print.

134 V. Linko, A. Ora and M. A. Kostiainen, *Trends Biotechnol.*, 2015, **33**, 586.

135 L. Liang, J.-W. Shen and Q. Wang, *Colloids Surf., B*, 2017, **153**, 168.

136 J. F. Rahbani, E. Vengut-Climent, P. Chidchob, Y. Gidi, T. Trinh, G. Cosa and H. F. Sleiman, *Adv. Healthcare Mater.*, 2018, **7**, 1701049.

137 A. M. Maier, W. Bae, D. Schiffels, J. F. Emmerig, M. Schiff and T. Liedl, *ACS Nano*, 2017, **11**, 1301.

138 S. Li, Q. Jiang, S. Liu, Y. Zhang, Y. Tian, C. Song, J. Wang, Y. Zou, G. J. Anderson, J.-Y. Han, Y. Chang, Y. Liu, C. Zhang, L. Chen, G. Zhou, G. Nie, H. Yan, B. Ding and Y. Zhao, *Nat. Biotechnol.*, 2018, **36**, 258.

139 W. Anderson, D. Kozak, V. A. Coleman, Å. K. Jämting and M. Trau, *J. Colloid Interface Sci.*, 2013, **405**, 322.

140 R. Finsy, *Adv. Colloid Interface Sci.*, 1994, **52**, 79.

141 R. A. Dragovic, C. Gardiner, A. S. Brooks, D. S. Tannetta, D. J. Ferguson, P. Hole, B. Carr, C. W. Redman, A. L. Harris, P. J. Dobson, P. Harrison and I. L. Sargent, *Nanomedicine*, 2011, **7**, 780.

142 V. Filipe, A. Hawe and W. Jiskoot, *Pharm. Res.*, 2010, **27**, 796.

143 C. Wu, M. Li, S. C. M. Kwan and G. J. Liu, *Macromolecules*, 1998, **31**, 7553.

144 D. E. Wagner, C. L. Phillips, W. M. Ali, G. E. Nybakken, E. D. Crawford, A. D. Schwab, W. F. Smith and R. Fairman, *PNAS*, 2005, **102**, 12656.

145 S. Sugihara, S. P. Armes, A. Blanazs and A. L. Lewis, *Soft Matter*, 2011, **7**, 10787.

146 B. Kavitha, K. Siva Kumar and N. Narsimlu, *Indian J. Pure Appl. Phys.*, 2013, **51**, 207.

147 A. D. Levin, E. A. Shmytkova and B. N. Khlebtsov, *J. Phys. Chem. C*, 2017, **121**, 3070.

148 T. Y. Ling, J. Wang and D. Y. H. Pui, International Aerosol Conference, St. Paul, September, 2006.

149 J. Gross, S. Sayle, A. R. Karow, U. Bakowsky and P. Garidel, *Eur. J. Pharm. Biopharm.*, 2016, **104**, 30.

150 P. Kramberger, M. Ciringer, A. Strancar and M. Peterka, *Virol. J.*, 2012, **9**, 1.

151 L. O. Narhi, Y. Jiang, S. Cao, K. Benedek and D. Shnek, *Curr. Pharm. Biotechnol.*, 2009, **10**, 373.

152 E. van der Pol, F. A. W. Coumans, A. E. Grootemaat, C. Gardiner, I. L. Sargent, P. Harrison, A. Sturk, T. G. van Leeuwen and R. Nieuwland, *J. Thromb. Haemostasis*, 2014, **12**, 1182.

153 J. G. Mehtala and A. Wei, *Langmuir*, 2014, **30**, 13737.

154 D. Mukhija and M. J. Solomon, *J. Colloid Interface Sci.*, 2007, **314**, 98.

155 F. Ruhnow, D. Zwicker and S. Diez, *Biophys. J.*, 2011, **100**, 2820.

156 W. Nasalski, *Trends in Mechanics of Materials*, IPPT PAN, Warszawa, 2007.

157 K. Visscher and M. J. Schnitzer, *Nature*, 1999, **400**, 184.

158 R. Huang, I. Chavez, K. M. Taute, B. Lukić, S. Jeney, M. G. Raizen and E. L. Florin, *Nat. Phys.*, 2011, **7**, 576.

159 Yogesha, S. Bhattacharya and S. Ananthamurthy, *Opt. Commun.*, 2012, **285**, 2530. Q20

160 A. Ashkin, *Phys. Rev. Lett.*, 1970, **24**, 156.

161 A. Ashkin, J. M. Dziedzic, J. E. Bjorkholm and S. Chu, *Opt. Lett.*, 1986, **11**, 288.

162 K. C. Neuman and A. Nagy, *Nat. Methods*, 2008, **5**, 491.

163 A. Yao, M. Tassieri, M. Padgett and J. Cooper, *Lab Chip*, 2009, **9**, 2568.

164 S. H. Simpson, *J. Quant. Spectrosc. Radiat. Transfer*, 2014, **146**, 81.

165 O. M. Maragò, P. H. Jones, P. G. Gucciardi, G. Volpe and A. C. Ferrari, *Nat. Nanotechnol.*, 2013, **8**, 807.

166 F. Hajizadeh, L. Shao, D. Andrén, P. Johansson, H. Rubinsztein-Dunlop and M. Käll, *Optica*, 2017, **4**, 746.

167 A. A. R. Neves, A. Camposeo, S. Pagliara, R. Saija, F. Borghese, P. Denti, M. A. Iatì, R. Cingolani, O. M. Maragò and D. Pisignano, *Opt. Express*, 2010, **18**, 822.

168 R. Huang, I. Chavez, K. M. Taute, B. Lukić, S. Jeney, M. G. Raizen and E.-L. Florin, *Nat. Phys.*, 2011, **7**, 576.

169 G. Boer, R. Johann, J. Rohner, F. Merenda, G. Delacrétaz, Ph. Renaud and R.-P. Salathé, *Rev. Sci. Instrum.*, 2007, **78**, 116101.

170 D. H. Ahmed and H. J. Sung, *Int. J. Optomechatron.*, 2012, **6**, 146.

171 F. Pierini, K. Zembrzycki, P. Nakielski, S. Pawłowska and T. A. Kowalewski, *Meas. Sci. Technol.*, 2016, **27**, 025904.